



Measurement of the exclusive $\gamma\gamma \rightarrow \mu^+\mu^-$ process in proton–proton collisions at $\sqrt{s} = 13$ TeV with the ATLAS detector

The ATLAS Collaboration*

ARTICLE INFO

Article history:

Received 15 August 2017
Received in revised form 13 December 2017
Accepted 13 December 2017
Available online 20 December 2017
Editor: W.-D. Schlatter

ABSTRACT

The production of exclusive $\gamma\gamma \rightarrow \mu^+\mu^-$ events in proton–proton collisions at a centre-of-mass energy of 13 TeV is measured with the ATLAS detector at the LHC, using data corresponding to an integrated luminosity of 3.2 fb^{-1} . The measurement is performed for a dimuon invariant mass of $12 \text{ GeV} < m_{\mu^+\mu^-} < 70 \text{ GeV}$. The integrated cross-section is determined within a fiducial acceptance region of the ATLAS detector and differential cross-sections are measured as a function of the dimuon invariant mass. The results are compared to theoretical predictions both with and without corrections for absorptive effects.

© 2017 The Author(s). Published by Elsevier B.V. This is an open access article under the CC BY license (<http://creativecommons.org/licenses/by/4.0/>). Funded by SCOAP³.

1. Introduction

When proton–proton (pp) beams collide at the LHC, typically rare photon–photon induced ($\gamma\gamma$) interactions occur at perceptible rate and provide a unique opportunity to study high-energy electroweak processes [1]. Compared to other final states, the dilepton production is a standard candle process of the photon-induced production mechanism, thanks to its sizeable cross-section. Using pp collisions at a centre-of-mass energy of $\sqrt{s} = 7$ TeV, measurements of $pp(\gamma\gamma) \rightarrow \mu^+\mu^-pp$ production (referred to as exclusive $\gamma\gamma \rightarrow \mu^+\mu^-$) were performed by the ATLAS and CMS collaborations [2,3]. The exclusive $\gamma\gamma \rightarrow e^+e^-$ process was also measured [3,4]. A similar experimental signature has been used to study the $\gamma\gamma \rightarrow W^+W^-$ reaction [5–7].

The exclusive $\gamma\gamma \rightarrow \mu^+\mu^-$ production process competes with the two-photon interactions involving single- or double-proton dissociation due to the virtual photon exchange (Fig. 1 (a–c)). The electromagnetic (EM) break-up of the proton typically results in a production of particles at small angles to the beam direction, which can mimic the exclusive process. However, the proton-dissociative processes have significantly different kinematic distributions compared to the exclusive reaction, allowing an effective separation of the different production mechanisms.

In general, the photon-induced production of lepton pairs contributes up to a few percent to the inclusive dilepton production at LHC energies [8–10].

In order to reproduce the data, the calculations of such photon-induced reactions, in particular exclusive $\gamma\gamma \rightarrow \mu^+\mu^-$ production, need to take into account the proton absorptive effects [3]. They are mainly related to additional gluon interactions between the protons (or proton remnants), shown in Fig. 1 (d), which take place in addition to the QED process. The size of the absorption is not expected to be the same for exclusive and dissociative processes; it may also depend on the reaction kinematics. These effects lead to the suppression of exclusive cross-sections (typically around 10–20%) by producing extra hadronic activity in the event besides the final-state muons. Recent phenomenological studies suggest that the exclusive cross-sections are suppressed, with a survival factor that decreases with mass [11,12].

In this paper, a measurement of exclusive dimuon production in pp collisions at $\sqrt{s} = 13$ TeV is presented for muon pairs with invariant mass $12 \text{ GeV} < m_{\mu^+\mu^-} < 70 \text{ GeV}$. The differential cross-sections, $d\sigma/dm_{\mu^+\mu^-}$, are determined within a fiducial acceptance region. In the region $30 \text{ GeV} < m_{\mu^+\mu^-} < 70 \text{ GeV}$, the minimum transverse momentum of each muon is required to be 10 GeV. For $12 \text{ GeV} < m_{\mu^+\mu^-} < 30 \text{ GeV}$, the minimum muon transverse momentum is reduced to 6 GeV by taking advantage of the lower trigger thresholds available by making additional requirements on muon-pair topology. In addition, both muons are measured in the pseudorapidity range of $|\eta^\mu| < 2.4$. The measurements are compared to theoretical predictions both with and without corrections for absorptive effects.

2. ATLAS detector

The ATLAS experiment [13] at the LHC is a multi-purpose particle detector with a forward–backward symmetric cylindrical ge-

* E-mail address: atlas.publications@cern.ch.

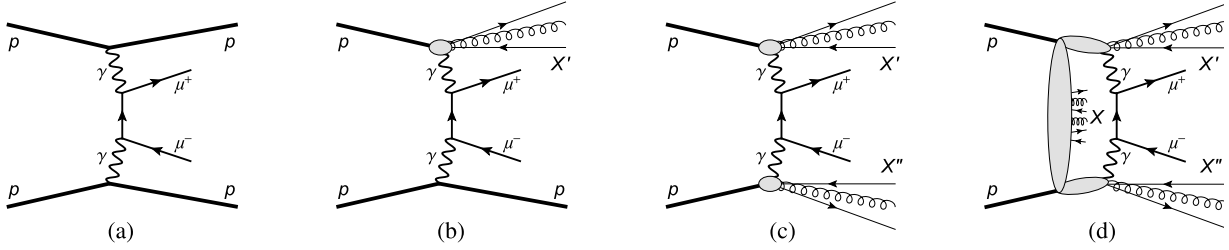


Fig. 1. Schematic diagrams for (a) exclusive, (b) single-proton dissociative and (c) double-proton dissociative two-photon production of muon pairs in pp collisions. The effect of additional interactions between the protons is shown in (d).

ometry and nearly 4π coverage in solid angle.¹ It consists of inner tracking devices surrounded by a superconducting solenoid, EM and hadronic calorimeters, and a muon spectrometer. The inner detector (ID) provides charged-particle tracking in the pseudorapidity region $|\eta| < 2.5$ and vertex reconstruction. It comprises a silicon pixel detector, a silicon microstrip tracker, and a straw-tube transition radiation tracker. The ID is surrounded by a solenoid that produces a 2 T axial magnetic field. Lead/liquid-argon (LAr) sampling calorimeters provide EM energy measurements with high granularity. A hadron (steel/scintillator-tile) calorimeter covers the central pseudorapidity range $|\eta| < 1.7$. The end-cap and forward regions are instrumented with LAr calorimeters for both the EM and hadronic energy measurements up to $|\eta| = 4.9$. The muon spectrometer (MS) is operated in a magnetic field provided by air-core superconducting toroids and includes tracking chambers for precise muon momentum measurements up to $|\eta| = 2.7$ and trigger chambers covering the range $|\eta| < 2.4$.

A two-level trigger system [14] selects the events used in the analysis. The first level is implemented in custom electronics, while the second trigger level is a flexible software-based system.

3. Data, simulated event samples and theoretical predictions

This analysis uses a data set of pp collisions collected at a centre-of-mass energy $\sqrt{s} = 13$ TeV during 2015 under stable beam conditions. After applying data quality requirements, this data sample corresponds to an integrated luminosity of 3.2 fb^{-1} .

Calculations of the cross-section for exclusive $\gamma\gamma \rightarrow \mu^+\mu^-$ production in pp collisions are based on the Equivalent Photon Approximation (EPA) [15,16]. The EPA relies on the property that the EM fields produced by the colliding protons can be treated as a beam of quasi-real photons with a small virtuality of $Q^2 < 0.1 \text{ GeV}^2$. This flux of equivalent photons is determined from the Fourier transform of the EM field of the proton, taking into account the EM form factors [17]. The cross-section for the reaction $pp(\gamma\gamma) \rightarrow \mu^+\mu^-pp$ is calculated by convolving the respective photon fluxes with the elementary cross-section for the process $\gamma\gamma \rightarrow \mu^+\mu^-$. The signal events for exclusive $\gamma\gamma \rightarrow \mu^+\mu^-$ production were generated using the HERWIG 7.0 [18,19] Monte Carlo (MC) event generator, in which the cross-section for the process is computed by combining the pp EPA with the leading-order (LO) formula for $\gamma\gamma \rightarrow \mu^+\mu^-$. It is found that the predictions for exclusive $\gamma\gamma \rightarrow \mu^+\mu^-$ production from HERWIG are identical to those from LPAIR 4.0 [20] generator.

The dominant background, photon-induced single-dissociative (S-diss) dimuon production (Fig. 1 (b)), was simulated using LPAIR 4.0 with the Brasse [21] and Suri-Yennie [22] structure functions for proton dissociation. For photon virtualities $Q^2 < 5 \text{ GeV}^2$ and masses of the dissociating system $m_N < 2 \text{ GeV}$, low-multiplicity states from the production and decays of Δ resonances are usually created. For higher Q^2 or m_N , the system decays into a variety of resonances, which produce a large number of forward particles. The LPAIR package was interfaced to JETSET 7.408 [23], where the LUND [24] fragmentation model is implemented.

The HERWIG and LPAIR generators do not include any corrections to account for proton absorptive effects. Hence the normalisation of these MC samples is further constrained by a data-driven procedure, as described in Section 6.

For double-dissociative (D-diss) reactions, PYTHIA 8.175 [25] was used with the NNPDF2.3QED [26] set of parton distribution functions (PDF). The NNPDF2.3QED set uses LO QED and next-to-next-to-leading-order (NNLO) perturbative QCD (pQCD) calculations to construct the photon PDF, starting from the initial scale $Q_0^2 = 2 \text{ GeV}^2$. Additionally, two alternative PDF sets, CT14QED [27] and LUXqed17 [28] are considered. Depending on the multiplicity of the dissociating system, the default PYTHIA 8 string or mini-string fragmentation model was used for proton dissociation. The absorptive effects in D-diss MC events are taken into account using the default multi-parton interactions model in PYTHIA 8 [29].

The NLO pQCD POWHEG-Box v2 [30–33] event generator was used with the CT10 [34] PDF to generate both the Drell-Yan (DY) $Z/\gamma^* \rightarrow \mu^+\mu^-$ and $Z/\gamma^* \rightarrow \tau^+\tau^-$ events. It was interfaced to PYTHIA 8.210 [25] applying the AZNLO [35] set of generator-parameter values (tune) for the modelling of non-perturbative effects, including the CTEQ6L1 [36] PDF set. The production of top-quark pair ($t\bar{t}$) events was also modelled using POWHEG-Box, interfaced to PYTHIA 6.428 [37]. The event generators used to model $Z/\gamma^* \rightarrow \mu^+\mu^-$, $Z/\gamma^* \rightarrow \tau^+\tau^-$ and $t\bar{t}$ reactions were interfaced to PHOTOS 3.52 [38,39] to simulate QED final-state radiation (FSR) corrections.

Multiple pp interactions per bunch crossing (pile-up) were accounted for by overlaying simulated minimum-bias events, generated with PYTHIA 8.210 using the A2 tune [40], and reweighting the distribution of the average number of interactions per bunch crossing in MC simulation to that observed in data. Furthermore, the simulated samples were weighted such that the z -position distribution of reconstructed pp interaction vertices matches the distribution observed in data. The ATLAS detector response was modelled using the GEANT4 toolkit [41,42] and the same event reconstruction as that used for data is performed.

The measured distribution of the exclusive $\gamma\gamma \rightarrow \mu^+\mu^-$ process is compared with two models of absorptive corrections in Section 8.

In the finite-size parameterisation approach [11], the absorptive effects are embedded in the evaluation of the $\gamma\gamma$ luminosity, taking the photon energy and impact parameter dependence into ac-

¹ ATLAS uses a right-handed coordinate system with its origin at the nominal interaction point in the centre of the detector and the z -axis coinciding with the axis of the beam pipe. The x -axis points from the interaction point to the centre of the LHC ring, and the y -axis points upward. The pseudorapidity is defined in terms of the polar angle θ as $\eta = -\ln \tan(\theta/2)$, and ϕ is the azimuthal angle around the beam pipe with respect to the x -axis. The angular distance is defined as $\Delta R = \sqrt{(\Delta\eta)^2 + (\Delta\phi)^2}$. The transverse momentum is defined relative to the beam axis.

count. A simple exponential form of the proton's transverse profile function, extracted from total and elastic pp and $p\bar{p}$ cross-section data, is used to suppress the two-photon luminosity when the impact parameter of the pp collision becomes small. It determines the probability that no inelastic interaction producing additional hadrons in the final state occurs [43]. Moreover, only photons produced outside the proton with an assumed radius of $r_p = 0.64$ fm are allowed to initiate the two-photon process. This particular feature reflects the finite transverse size of the proton and leads to further suppression of the cross-section.

In the approach implemented in the SUPERCHIC2 event generator [12], the absorptive effects are included at the amplitude level differentially in the final-state momenta of scattered protons. As a result, the suppression of the cross-section in general depends on the helicity structure of the $\gamma\gamma \rightarrow X$ sub-process and may also alter the kinematics of outgoing intact protons. Because some helicity amplitudes vanish for the $\gamma\gamma \rightarrow \mu^+\mu^-$ process in the limit of massless leptons, this effect plays a less significant role in the suppression of the $pp(\gamma\gamma) \rightarrow \mu^+\mu^-pp$ cross-section. As in the model described above, the proton transverse profile function controls the reduction of the exclusive production cross-section when pp collisions become central. It is fitted using a two-channel eikonal model to describe a range of total, elastic and diffractive pp and $p\bar{p}$ data [44].

4. Event reconstruction, baseline selection and background estimation

Events were selected online by a set of dimuon triggers with a muon p_T threshold of 6 GeV or 10 GeV, and dimuon invariant mass $10 \text{ GeV} < m_{\mu^+\mu^-} < 30 \text{ GeV}$ or $m_{\mu^+\mu^-} > 30 \text{ GeV}$ respectively. Triggers with the lower transverse momentum requirement were enabled for data-taking with an instantaneous luminosity below $1.2 \times 10^{34} \text{ cm}^{-2} \text{ s}^{-1}$. These triggers were designed to collect exclusive dimuon events by employing an additional selection on the transverse momentum of the dimuon system, $p_T^{\mu^+\mu^-} < 2 \text{ GeV}$, to reduce contributions from DY and multijet production.

In each event, muon candidates are identified by matching complete tracks in the MS to tracks in the ID and are required to be in the region $|\eta^\mu| < 2.4$. The *Medium* criterion, as defined in Ref. [45], is applied to the combined tracks. The muons are required to be isolated using information from ID tracks and calorimeter energy clusters in a cone around the muon using the so-called *GradientLoose* criteria [45]. For each muon, the significance of the transverse impact parameter, defined by the transverse impact parameter (d_0) of a muon track with respect to the beam line divided by its estimated uncertainty (σ_{d_0}), is required to satisfy $|d_0|/\sigma_{d_0} < 3.0$.

Events are then required to have exactly one pair of oppositely-charged muons. Muons are required to form a pair with an invariant mass of $12 \text{ GeV} < m_{\mu^+\mu^-} < 30 \text{ GeV}$ or $m_{\mu^+\mu^-} > 30 \text{ GeV}$ with different p_T^μ conditions. The offline p_T^μ requirements are identical to the trigger-level requirements, since the trigger efficiencies are found to be constant in the relevant p_T^μ range. Each of the two muons must also be matched to one of the muons reconstructed by the trigger.

In order to select exclusive events, the average longitudinal impact parameter of the two leptons is taken as the event vertex and is referred to as the dimuon vertex. The longitudinal impact parameter of each muon track with respect to the dimuon vertex multiplied by the sine of the track θ angle, is required to be less than 0.5 mm.

After these baseline selection requirements, 2.9×10^6 dimuon candidates are found in the data.

The background to the exclusive signal includes contributions from S-diss and D-diss $\gamma\gamma \rightarrow \mu^+\mu^-$ production, as well as $Z/\gamma^* \rightarrow \mu^+\mu^-$ or $Z/\gamma^* \rightarrow \tau^+\tau^-$, with less significant contamination due to $t\bar{t}$ and multijet production. S-diss and D-diss background contributions are estimated using MC simulation, with additional data-driven normalisation of the S-diss contribution as detailed in Section 6. The Z/γ^* and $t\bar{t}$ background contributions are also estimated from simulation, and normalised using the respective inclusive cross-sections calculated at NNLO in perturbative QCD [46,47]. The background from $\gamma\gamma \rightarrow W^+W^-$ and $\gamma\gamma \rightarrow \tau^+\tau^-$ processes contributes at a level below 0.2% of the expected signal [7] and is therefore neglected. The background contribution from W + jets production is also estimated to be negligible [8]. Scale factors are applied to the simulated samples to correct for the small differences between simulation and data in the muon trigger, reconstruction and identification efficiencies, as well as the momentum scale and resolution [45]. The efficiencies are measured using a tag-and-probe method combining results from $J/\psi \rightarrow \mu^+\mu^-$, $\Upsilon \rightarrow \mu^+\mu^-$, and $Z \rightarrow \mu^+\mu^-$ events to cover a large range in the muon transverse momentum.

The multijet background is determined using data-driven methods, similarly to the previous ATLAS exclusive dilepton measurement [3]. It is extracted using same-charge muon pairs that satisfy the event selection criteria, except the requirement on muon charge. The normalisation of the multijet background is determined by fitting the invariant mass spectrum of the muon pair in the data to the sum of expected contributions, including MC predictions of the signal and the prompt muon backgrounds.

5. Exclusive selection

A typical signature of exclusive $\gamma\gamma \rightarrow \mu^+\mu^-$ events is the absence of charged-particle tracks, other than muon tracks [3,7]. In contrast, inclusive background candidates (like DY or multijet) are produced with extra particles that originate from the emission and hadronisation of additional partons [48,49]. Therefore, in order to select exclusive $\gamma\gamma \rightarrow \mu^+\mu^-$ candidates, a veto on additional charged-particle track activity is applied. This vertex isolation requires no additional tracks with $p_T > 400 \text{ MeV}$ and $|\eta| < 2.5$ near the dimuon vertex with $|z_0^{\text{trk}}| < 1 \text{ mm}$, where z_0^{trk} is the longitudinal impact parameter of track with respect to the dimuon vertex. The value of 1 mm is optimised using the MC simulation and the expected signal significance. This value is identical to that used in Ref. [7].

Following the procedure described in Refs. [3,48], the shape of the charged-particle multiplicity distribution in simulated DY events is reweighted to match the spectrum observed in data. The uncorrected Z/γ^* model overestimates the charged-particle spectrum observed in data by 50% for low-multiplicity events. In order to estimate the relevant weights, the events in the Z -mass region (defined as $70 \text{ GeV} < m_{\mu^+\mu^-} < 105 \text{ GeV}$) are used, since this region is expected to include a large DY contribution. The distribution of the number of tracks associated with the dimuon vertex after applying the charged-particle reweighting procedure to DY simulation is shown in Fig. 2 (a) for events in the Z -mass region. A small mismodelling of this distribution is due to the contribution from fake tracks and secondary particles [48], not taken into account in the correction procedure. Similarly to Ref. [50], the underlying event activity in DY events is found to be independent of the dimuon invariant mass, down to $m_{\mu^+\mu^-} = 12 \text{ GeV}$. For this reason, the same weights are applied to simulated DY events outside the Z -mass region (Fig. 2 (b)), and the description of charged-particle multiplicity is found to be satisfactory. To cover differences observed between the data and simulation, a 10% global uncer-

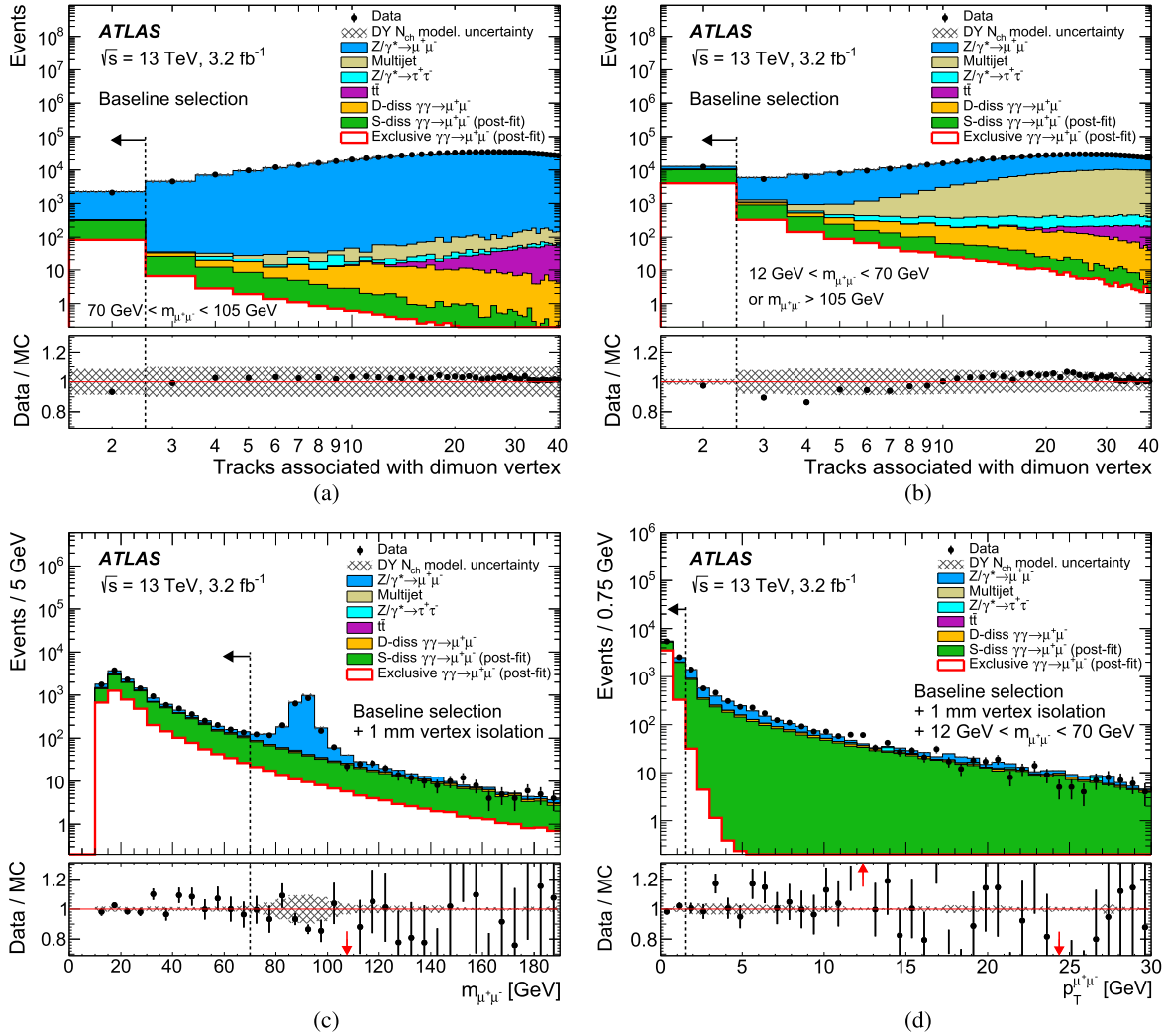


Fig. 2. Illustration of event selection. The distribution of the number of charged-particle tracks at detector level after applying the charged-particle reweighting procedure to DY MC simulation for (a) the Z-mass region and (b) the invariant mass range outside the Z-mass region. (c) Dimuon invariant mass ($m_{\mu^+\mu^-}$) distribution after applying 1 mm vertex isolation. (d) Transverse momentum of the dimuon system ($p_T^{\mu^+\mu^-}$) distribution after applying 1 mm vertex isolation and requiring $m_{\mu^+\mu^-} < 70$ GeV. Data are shown as points with statistical error bars, while the histograms represent the expected signal and background levels. The dashed vertical lines and arrows indicate the signal region selection. The uncertainty band indicates 10% global uncertainty applied to DY simulation due to charged-particle multiplicity modelling. The exclusive and S-diss yields are corrected using the fit procedure described in the text. The lower panels show the ratio of data to expected event yields. Red arrows in the lower panels indicate bins where the corresponding entry falls outside the plotted range. (For interpretation of the references to colour in this figure legend, the reader is referred to the web version of this article.)

Table 1

Effect of sequential selection requirements on the number of events observed in data, compared to the numbers of predicted signal and background events.

| | Data | Signal | Total background | S-diss | D-diss | $Z/\gamma^* \rightarrow \mu^+\mu^-$ | $Z/\gamma^* \rightarrow \tau^+\tau^-$ | Multijet | $t\bar{t}$ |
|------------------------------|-----------|--------|------------------|--------|--------|-------------------------------------|---------------------------------------|----------|------------|
| Baseline selection | 2 933 384 | 5740 | 2 897 000 | 8640 | 8000 | 2 268 000 | 10900 | 590 000 | 12 200 |
| 1 mm vertex isolation | 14 759 | 4560 | 11 100 | 6840 | 300 | 3900 | 30 | 50 | 0 |
| $m_{\mu^+\mu^-} < 70$ GeV | 12 395 | 4420 | 8800 | 6420 | 300 | 2000 | 30 | 50 | 0 |
| $p_T^{\mu^+\mu^-} < 1.5$ GeV | 7952 | 4370 | 4300 | 3550 | 60 | 670 | 7 | 10 | 0 |

tainty is assigned to DY MC simulation due to charged-particle multiplicity modelling.

The invariant mass distribution of muon pairs for events satisfying the 1 mm vertex isolation is presented in Fig. 2 (c). The contribution from DY events is further reduced by including only events with a dimuon invariant mass below 70 GeV. In order to further suppress the background from the S-diss process, the muon pair is required to have a transverse momentum, $p_T^{\mu^+\mu^-}$, below 1.5 GeV. This is presented in Fig. 2 (d).

Table 1 presents the effect of each step of the selection on the data and the expected numbers of signal and background events.

6. Cross-section measurements

As in the previous ATLAS measurement [3], the exclusive $\gamma\gamma \rightarrow \mu^+\mu^-$ contribution is extracted by performing a binned maximum-likelihood fit to the measured dimuon acoplanarity ($1 - |\Delta\phi_{\mu^+\mu^-}|/\pi$) distribution. The acoplanarity variable is not af-

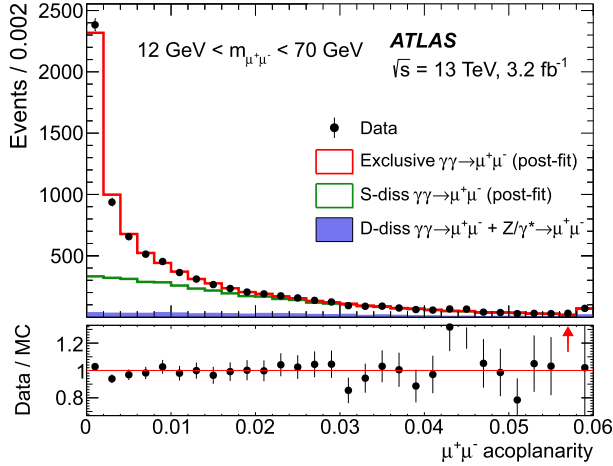


Fig. 3. Dimuon acoplanarity distribution after signal selection requirements. Data are shown as points with statistical error bars, while the histograms, in top-to-bottom order, represent the simulated exclusive signal, the S-diss and the sum of D-diss and DY backgrounds. The exclusive and S-diss yields are determined from the fit described in the text. The last bin includes overflow events. The lower panel shows the ratio of data to the predicted distribution. Red arrow in the lower panel indicates a bin where the corresponding entry falls outside the plotted range. (For interpretation of the references to colour in this figure legend, the reader is referred to the web version of this article.)

Table 2
Definition of the fiducial region for which the cross-sections are evaluated.

| Invariant mass range | p_T^μ requirement | $ \eta^\mu $ requirement |
|------------------------------------|-----------------------|--------------------------|
| 12 GeV < $m_{\mu^+\mu^-}$ < 30 GeV | > 6 GeV | < 2.4 |
| 30 GeV < $m_{\mu^+\mu^-}$ < 70 GeV | > 10 GeV | < 2.4 |

affected by the muon momentum scale and resolution uncertainties and provides a good separation of signal from background. Templates from MC simulation are used for the signal, DY, S-diss and D-diss processes. Contributions from other background sources are found to be negligible. The fit determines two parameters: the expected number of signal events and the expected number of S-diss events. The D-diss and DY contributions are fixed to their corresponding MC predictions in the fit procedure.

The dimuon acoplanarity distribution in data overlaid with the result of the fit to the shapes from MC simulation is shown in Fig. 3 for the fiducial region.

The cross-section measurements presented here correspond to the fiducial region defined in Table 2. The fiducial cross-section for the process $pp(\gamma\gamma) \rightarrow \mu^+\mu^-pp$ is determined according to

$$\sigma_{\gamma\gamma \rightarrow \mu^+\mu^-}^{\text{excl. fid.}} = \frac{N_{\text{excl.}}}{L_{\text{int}} \times C},$$

where $N_{\text{excl.}}$ is the total number of signal events extracted using the log-likelihood fit procedure, L_{int} is the integrated luminosity of the data sample and C is the overall correction factor that accounts for efficiencies and resolution effects. The C factor is defined as the ratio of the number of reconstructed MC signal events passing the selection to the number of generated MC signal events satisfying the fiducial requirements.

The cross-section for exclusive dimuon production is also measured differentially in four bins of $m_{\mu^+\mu^-}$ from 12 GeV to 70 GeV. The bin widths are chosen to ensure purity above 90%, where purity is defined as the fraction of reconstructed signal events in a given bin of $m_{\mu^+\mu^-}$ which were also generated in the same bin. The differential measurement is unfolded for resolution effects using the signal simulation sample and a bin-by-bin correction pro-

cedure. The differential fiducial cross-section as a function of the dimuon invariant mass is calculated as

$$\left(\frac{d\sigma_{\gamma\gamma \rightarrow \mu^+\mu^-}^{\text{excl.}}}{dm_{\mu^+\mu^-}} \right)_i = \frac{N_{\text{excl.}}^i}{L_{\text{int}} \times C_i \times (\Delta m)_i}, \quad (1)$$

where $N_{\text{excl.}}^i$ is the number of signal events recorded in the i -th invariant mass bin, C_i is the correction factor in bin i and $(\Delta m)_i$ is the width of the bin.

7. Systematic uncertainties

The systematic uncertainties in the measurement enter the cross-sections determination through the calculation of the correction factors (C_i), the extracted number of signal events ($N_{\text{excl.}}^i$), or the estimation of L_{int} .

The systematic uncertainties are classified as correlated or uncorrelated across the measurement bins. The correlated contributions are propagated by the offset method in which the values from each source are coherently shifted upwards and downwards by one standard deviation and the magnitude of the change in the measurement is computed. The sign of the uncertainty corresponds to a one standard deviation upward shift of the uncertainty source. The uncorrelated sources are propagated using the pseudo-experiment method in which the correction factors used to improve the modelling of data by the simulation are randomly shifted in an ensemble of pseudo-experiments according to the mean and standard deviation of the correction factor. The resulting uncertainty in the measured cross-sections is determined from the variance of the measurements for the ensemble.

Muon-related sources: Uncertainties related to the muon trigger and selection efficiencies are studied using the $J/\psi \rightarrow \mu^+\mu^-$, $\Upsilon \rightarrow \mu^+\mu^-$ and $Z \rightarrow \mu^+\mu^-$ processes, and a tag-and-probe method [14].

The muon trigger efficiency is estimated in simulation, with a dedicated data-driven analysis performed to obtain the simulation-to-data correction factors and the corresponding uncertainties. The uncertainty in the correction factors C_i in Eqn. (1) due to the statistical ($\delta_{\text{stat.}}^{\text{trig.}}$) and systematic ($\delta_{\text{syst.}}^{\text{trig.}}$) uncertainties in the trigger efficiency are around 0.3% and 0.9% respectively.

The muon selection efficiencies as determined from simulation are corrected with simulation-to-data correction factors, which have associated statistical and systematic uncertainties. These contributions to the systematic uncertainty also affect C_i , and are denoted by $\delta_{\text{stat.}}^{\text{reco.}}$ and $\delta_{\text{syst.}}^{\text{reco.}}$ respectively. The $\delta_{\text{stat.}}^{\text{reco.}}$ value is approximately 0.1% and the $\delta_{\text{syst.}}^{\text{reco.}}$ value is around 1.0%.

Uncertainties in the muon momentum calibration can cause a change of acceptance because of migration of events across the muon p_T thresholds and $m_{\mu^+\mu^-}$ boundaries. They are obtained from a comparison of the J/ψ and Z boson invariant mass distributions in data and simulation [45]. When propagated to the correction factors, this source is found to be below 0.5%. This contribution is denoted by $\delta_{\text{sc./res.}}$.

Vertex isolation efficiency: Since the dimuon vertex in each event occurs randomly within the Gaussian luminous region, the 1 mm dimuon vertex isolation efficiency is extracted from the data as follows: for each event i , a point z_i is randomly chosen from a Gaussian distribution corresponding to the longitudinal shape of the luminous region, excluding a range of 20 mm centred about the dimuon vertex. This region is excluded to ensure any activity around point z_i is unrelated to the dimuon vertex. In some events, the point z_i is near tracks

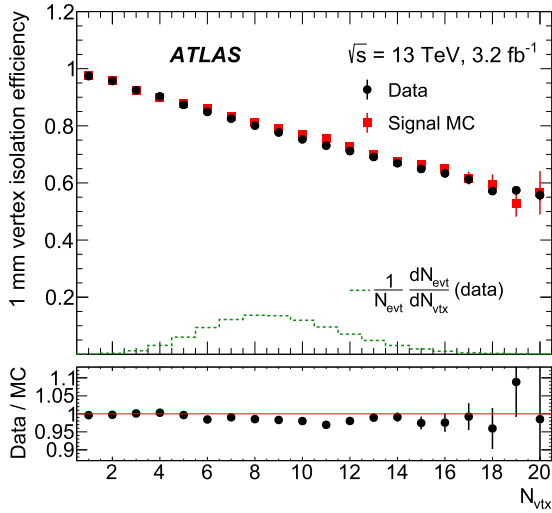


Fig. 4. Dimuon vertex isolation efficiency for 1 mm requirement extracted from the data (black points) and signal MC simulation (red squares) as a function of the number of reconstructed vertices N_{vtx} . The distribution in the data is built according to the procedure described in the text. The normalised N_{vtx} distribution for data is shown as the dashed histogram. (For interpretation of the references to colour in this figure legend, the reader is referred to the web version of this article.)

caused e.g. by pile-up interactions. The vertex isolation efficiency is defined as the fraction of events for which z_i has no track within 1 mm. This efficiency, as measured in data, is compared with simulation in Fig. 4 as a function of the number of reconstructed vertices (N_{vtx}). The average number of reconstructed vertices per event observed in data is approximately 9. In general, good agreement between the data and simulation is observed, with a small systematic difference of 1–2% observed in the region $8 < N_{\text{vtx}} < 12$, which impacts the C_i by 1.1% and this is taken as a systematic uncertainty. It was also checked that the vertex isolation efficiency is well modelled by simulation for arbitrary choice of vertex isolation size.

Modelling of the muon impact parameter resolution may affect the vertex isolation efficiency and can give rise to additional systematic effects. This is estimated by varying the muon impact parameter resolution in simulation to match the shapes observed in data, and the impact on the cross-sections is found to be 0.3%.

In total, the resulting uncertainty in the correction factors due to estimation of the vertex isolation efficiency is found to be $\delta^{\text{veto}} = 1.2\%$.

Pile-up description: The systematic effect related to the pile-up modelling is estimated from the comparison between data and simulation of the p_T - and η -dependent density of tracks originating from pile-up, as in Refs. [3,48]. The resulting uncertainty in C_i is found to be $\delta^{\text{PU}} = 0.5\%$ and is fully correlated with the δ^{veto} .

Background: The uncertainty in the contribution of the DY process mainly accounts for disagreement between the data and simulation in charged-particle multiplicity modelling (10%). It also includes a 5% contribution due to the PDF and scale uncertainties [51]. An overall normalisation uncertainty of 20% is assigned to cover these effects. Because of the similar shapes of the DY and S-diss $\gamma\gamma \rightarrow \mu^+\mu^-$ components in the fitted acoplanarity distribution, the uncertainty in the DY normalisation is partly absorbed by the S-diss contribution. The 20% uncertainty has typically a 0.7% effect on the extracted number of signal events.

In order to estimate the D-diss $\gamma\gamma \rightarrow \mu^+\mu^-$ uncertainty, this contribution is varied according to the photon PDF uncertainties, defined at 68% confidence level and evaluated using NNPDF2.3QED replicas [26]. The D-diss background uncertainty produces an uncertainty of 0.2% in the cross-sections, which is consistent with the full difference between the predictions obtained with the NNPDF2.3QED, CT14QED [27] and LUXqed17 [28] central values.

The impact of these two background uncertainty sources is added in quadrature, yielding the uncertainty in N_{excl}^i ($\delta^{\text{bkg.}}$), which is less than 0.8%.

Template shape: The default signal acoplanarity template is constructed using bare EPA predictions from HERWIG. When using the acoplanarity templates from SUPERCHIC2 or from Ref. [11], the extracted number of signal events is lower by 2–3%, which is taken as a systematic uncertainty. The impact of the proton elastic form-factor modelling on the signal acoplanarity template is evaluated in a similar way to Ref. [3] and takes into account differences between various parameterisations of proton EM form factors. This has a 0.4% effect on the extracted number of signal events.

The impact of the shape uncertainty in the S-diss template is evaluated by varying the $p_T^{\mu^+\mu^-}$ requirement between 1 GeV and 2 GeV. The maximum deviation of N_{excl}^i from the nominal value is observed to be 0.8% and is taken as a systematic uncertainty. In order to assign uncertainty due to the choice of proton structure functions in LPAIR, an alternative set from Ref. [52] is used. This impacts the N_{excl}^i by about 2.0% and is taken as a systematic uncertainty.

When added in quadrature, these contributions are listed as δ_{shapes} .

LHC beam effects: The impact of the non-zero crossing angles of the LHC beams at the ATLAS interaction point is estimated by applying a Lorentz transformation to the generator-level lepton kinematics for signal MC events. This results in a negligible variation of the cross-sections. The LHC beam energy uncertainty is estimated to be 0.1% [53]. It affects the cross-sections by less than 0.1% and is considered to be a negligible effect.

Unfolding method: The bin-by-bin correction used in the calculation of the cross-sections is compared to an iterative Bayesian unfolding technique [54]. The differences between these two approaches are found to be negligible.

Luminosity: The uncertainty in L_{int} is estimated to be $\delta^{\text{lumi.}} = 2.1\%$. It is derived, following a methodology similar to that detailed in Ref. [55], from a calibration of the luminosity scale using x–y beam-separation scans performed in August 2015.

Other cross-checks: To check the impact of MC modelling of neutral particles in the background processes, the analysis is repeated at generator level by requiring no extra neutral particle with $p_T > 400$ MeV and $|\eta| < 2.5$, in addition to the charged-particle exclusive selection. This extra requirement shows negligible impact on the analysis.

In similar generator-level studies, the p_T threshold for charged particles is lowered to 100 MeV. The MC event yields for the dominant S-diss and a smaller D-diss background processes remain unchanged. For DY background the yield is suppressed by 80%. No additional systematic uncertainty is, however, assigned as the DY contribution is constrained using Z-mass control region for a nominal selection with a total uncertainty of 20%.

A summary of all systematic uncertainties is given in Table 3.

Table 3

The measured exclusive $\gamma\gamma \rightarrow \mu^+\mu^-$ differential fiducial cross-sections, $d\sigma/dm_{\mu^+\mu^-}$. The extracted number of signal events ($N_{\text{excl.}}^i$) and correction factors (C_i) are also shown. The measurements are listed together with the statistical ($\delta^{\text{stat.}}$), and total systematic ($\delta^{\text{syst.}}$) uncertainties. In addition, the contributions from the individual correlated and uncorrelated systematic error sources are provided. The last row lists $d\sigma/dm_{\mu^+\mu^-}$ in the total fiducial region. The uncertainties in $N_{\text{excl.}}^i$ correspond to the combined statistical and systematic uncertainties. These are correlated across $m_{\mu^+\mu^-}$ bins.

| $m_{\mu^+\mu^-}$ [GeV] | $N_{\text{excl.}}^i$ | C_i | $d\sigma/dm_{\mu^+\mu^-}$ [pb/GeV] | $\delta^{\text{stat.}}$ [%] | $\delta^{\text{syst.}}$ [%] | Uncorrelated | | Correlated | | | | | | | |
|---------------------------|----------------------|---------------|---------------------------------------|--------------------------------|--------------------------------|--------------------------------------|--------------------------------------|--------------------------------------|--------------------------------------|-----------------------------------|-------------------------------|-----------------------------|-------------------------------|---------------------------------|--------------------------------|
| | | | | | | $\delta^{\text{trig. stat.}}$ [%] | $\delta^{\text{reco. stat.}}$ [%] | $\delta^{\text{trig. syst.}}$ [%] | $\delta^{\text{reco. syst.}}$ [%] | $\delta^{\text{sc./res.}}$ [%] | δ^{veto} [%] | δ^{PU} [%] | $\delta^{\text{bkg.}}$ [%] | δ^{shapes} [%] | $\delta^{\text{lumi.}}$ [%] |
| 12–17 | 1290 ± 60 | 0.333 ± 0.007 | 0.243 ± 0.013 | 3.4 | 4.3 | 0.3 | 0.1 | 0.9 | 0.9 | −0.4 | −1.2 | −0.5 | 0.8 | 3.0 | 2.1 |
| 17–22 | 1040 ± 50 | 0.398 ± 0.008 | 0.164 ± 0.010 | 3.7 | 4.5 | 0.3 | 0.1 | 0.9 | 1.0 | −0.4 | −1.2 | −0.5 | 0.8 | 3.3 | 2.1 |
| 22–30 | 830 ± 40 | 0.428 ± 0.009 | 0.076 ± 0.005 | 3.9 | 4.6 | 0.2 | 0.1 | 0.9 | 1.0 | −0.2 | −1.2 | −0.5 | 0.6 | 3.5 | 2.1 |
| 30–70 | 690 ± 40 | 0.416 ± 0.008 | 0.013 ± 0.001 | 4.9 | 4.9 | 0.3 | 0.1 | 1.0 | 1.1 | −0.3 | −1.2 | −0.5 | 0.4 | 4.0 | 2.1 |
| 12–70 | 3850 ± 160 | 0.387 ± 0.008 | 0.054 ± 0.003 | 2.1 | 4.5 | 0.3 | 0.1 | 0.9 | 1.0 | −0.3 | −1.2 | −0.5 | 0.8 | 3.3 | 2.1 |

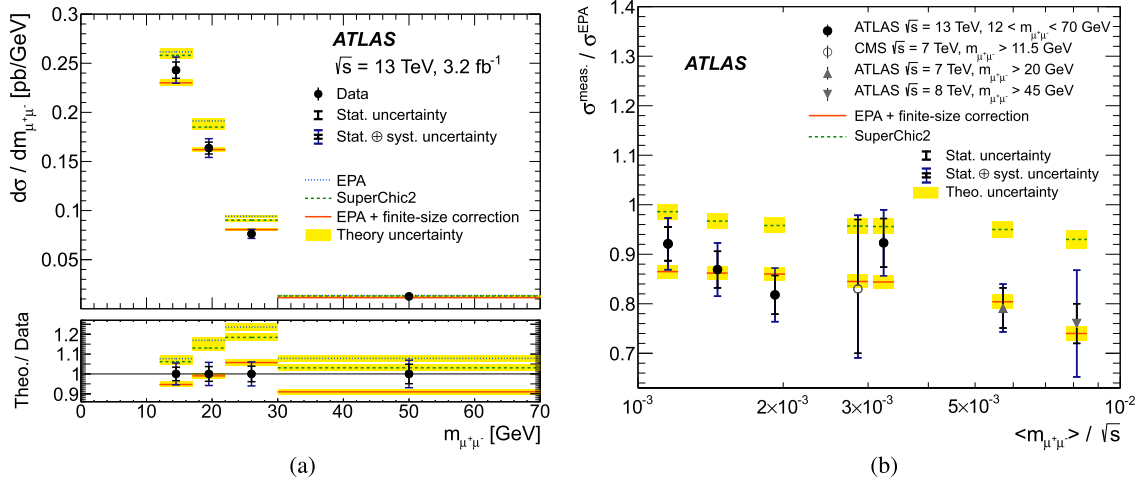


Fig. 5. (a) The exclusive $\gamma\gamma \rightarrow \mu^+\mu^-$ differential fiducial cross-section measurements as a function of dimuon invariant mass $m_{\mu^+\mu^-}$. (b) Comparison of the ratios of measured and predicted cross-sections to the bare EPA calculations as a function of the average dimuon invariant mass scaled to the pp centre-of-mass energy used. Data (markers) are compared to various predictions (lines). Full circle markers represent the four mass points presented in this paper, while open circle, up-triangle and down-triangle depict the previous results obtained with $m_{\mu^+\mu^-} > 11.5$ GeV [2], $m_{\mu^+\mu^-} > 20$ GeV [3] and $m_{\mu^+\mu^-} > 45$ GeV [7] requirements on the dimuon invariant mass. The inner error bars represent the statistical uncertainties, and the outer bars represent the total uncertainty in each measurement. The yellow bands represent the theoretical uncertainty in the predictions. The bottom panel in (a) shows the ratio of the predictions to the data. (For interpretation of the references to colour in this figure legend, the reader is referred to the web version of this article.)

8. Results

The fiducial cross-section is measured to be

$$\sigma_{\gamma\gamma \rightarrow \mu^+\mu^-}^{\text{excl. fid.}} = 3.12 \pm 0.07 (\text{stat.}) \pm 0.14 (\text{syst.}) \text{ pb.}$$

This value can be compared to the bare EPA predictions from HERWIG, $\sigma_{\gamma\gamma \rightarrow \mu^+\mu^-}^{\text{EPA}} = 3.56 \pm 0.05$ pb, to the EPA predictions corrected for absorptive effects using the finite-size parameterisation, $\sigma_{\gamma\gamma \rightarrow \mu^+\mu^-}^{\text{EPA, corr.}} = 3.06 \pm 0.05$ pb, or to the SUPERCHIC2 predictions, $\sigma_{\gamma\gamma \rightarrow \mu^+\mu^-}^{\text{SC2}} = 3.45 \pm 0.05$ pb. The theory uncertainties include uncertainties related to the knowledge of proton elastic form factors (1.5%), and those originating from the higher-order electroweak corrections [56] not included in the calculations (0.7%). These uncertainties are evaluated in a similar way as in Ref. [3].

The measured differential fiducial cross-sections as a function of dimuon invariant mass, together with the breakdown of the systematic uncertainties for the correlated and uncorrelated sources, are given in Table 3. The comparison between the measured cross-sections and the theoretical predictions is shown in Fig. 5 (a). The EPA predictions corrected for absorptive effects are in good agreement with the measured cross-sections. The total systematic uncertainty of the measurement is dominated by shape modelling uncertainties, which can be reduced by tagging outgoing protons with dedicated forward detectors [57,58].

It is expected that absorptive effects in two-photon interactions in pp collisions depend on the proton energy fractions passed to the quasi-real photons (denoted by x_1 and x_2) [11,12]. Therefore, it is interesting to study the evolution of the survival factor, defined as the ratio of measured cross-section to the bare EPA predictions, as a function of the average dimuon invariant mass. Indeed, since $m_{\mu^+\mu^-}^2/s = x_1x_2$, where s is the pp centre-of-mass energy squared, the average values can be obtained:

$$\langle x \rangle \approx \langle m_{\mu^+\mu^-} \rangle / \sqrt{s},$$

since at mid-rapidity ($y_{\mu^+\mu^-} \approx 0$) one has $x_1 \approx x_2$.

Fig. 5 (b) shows the evolution of the survival factor as a function of the average dimuon invariant mass scaled by a given pp centre-of-mass energy. Exclusive two-photon production of muon pairs in pp collisions at the LHC has been studied by the CMS experiment at $\sqrt{s} = 7$ TeV for $m_{\mu^+\mu^-} > 11.5$ GeV [2]. The ATLAS experiment measured exclusive production of muons at $\sqrt{s} = 7$ TeV in the region $m_{\mu^+\mu^-} > 20$ GeV [3]. Recently the production of exclusive $\gamma\gamma \rightarrow \mu^+\mu^-$ at $\sqrt{s} = 8$ TeV was also studied by ATLAS in the context of exclusive $\gamma\gamma \rightarrow W^+W^-$ measurement [7]. The probed invariant mass region in this case is $m_{\mu^+\mu^-} > 45$ GeV. The $\langle m_{\mu^+\mu^-} \rangle$ for different measurements is calculated using the HERWIG generator and corresponding fiducial region definitions. The deviations from unity of the ratios of measured cross-sections to the bare EPA-based predictions from HERWIG increase slightly with

the energy scale $\langle m_{\mu^+\mu^-} \rangle / \sqrt{s}$. This indicates that the size of the absorptive corrections tends to increase with $\langle m_{\mu^+\mu^-} \rangle / \sqrt{s}$.

The measurements are also compared to two model predictions that differ in the implementation of the absorptive corrections. While the finite-size parameterisation of absorptive effects describes the data reasonably well, mismodelling at the level of 10–20% is observed with SUPERCHIC2. Moreover, at large masses, SUPERCHIC2 predicts less steeper decrease of the survival factor as a function of $\langle x \rangle$. For example, the survival factor for fully exclusive $\gamma\gamma \rightarrow W^+W^-$ production at $\sqrt{s} = 13$ TeV is 0.82 [12] or 0.65 [11], respectively. A larger suppression of the EPA cross-sections in the finite-size approach is obtained by requiring that only photons outside the proton (with $r_p = 0.64$ fm) can initiate the exclusive photon-induced process.

9. Summary

A measurement of the cross-sections for exclusive $\gamma\gamma \rightarrow \mu^+\mu^-$ production in pp collisions at $\sqrt{s} = 13$ TeV with the ATLAS detector at the LHC is presented. The measurement uses a data set corresponding to an integrated luminosity of 3.2 fb^{-1} . The fiducial cross-section in the dimuon invariant mass range of $12 \text{ GeV} < m_{\mu^+\mu^-} < 70 \text{ GeV}$ is measured to be $\sigma_{\gamma\gamma \rightarrow \mu^+\mu^-}^{\text{excl. fid.}} = 3.12 \pm 0.07 \text{ (stat.)} \pm 0.14 \text{ (syst.) pb}$. The differential cross-sections as a function of the dimuon invariant mass are also measured.

The cross-sections are compared to theoretical predictions which include corrections for absorptive effects. The finite-size parameterisation of absorptive corrections provides a good description of the data, yielding $\sigma_{\gamma\gamma \rightarrow \mu^+\mu^-}^{\text{excl. fid.}} = 3.06 \pm 0.05 \text{ pb}$. It is observed that the absorptive corrections tend to increase with the energy fraction of protons passed to the initial-state photons. The precision of the measurement can be improved by using dedicated forward proton detectors.

Acknowledgements

We thank CERN for the very successful operation of the LHC, as well as the support staff from our institutions without whom ATLAS could not be operated efficiently.

We acknowledge the support of ANPCyT, Argentina; YerPhI, Armenia; ARC, Australia; BMWFW and FWF, Austria; ANAS, Azerbaijan; SSTC, Belarus; CNPq and FAPESP, Brazil; NSERC, NRC and CFI, Canada; CERN; CONICYT, Chile; CAS, MOST and NSFC, China; COLCIENCIAS, Colombia; MSMT CR, MPO CR and VSC CR, Czech Republic; DNRF and DNSRC, Denmark; IN2P3-CNRS, CEA-DRF/IRFU, France; SRNSF, Georgia; BMBF, HGF, and MPG, Germany; GSRT, Greece; RGC, Hong Kong SAR, China; ISF, I-CORE and Benoziyo Center, Israel; INFN, Italy; MEXT and JSPS, Japan; CNRST, Morocco; NWO, Netherlands; RCN, Norway; MNiSW and NCN, Poland; FCT, Portugal; MNE/IFA, Romania; MES of Russia and NRC KI, Russian Federation; JINR; MESTD, Serbia; MSSR, Slovakia; ARRS and MIZŠ, Slovenia; DST/NRF, South Africa; MINECO, Spain; SRC and Wallenberg Foundation, Sweden; SERI, SNSF and Cantons of Bern and Geneva, Switzerland; MOST, Taiwan; TAEK, Turkey; STFC, United Kingdom; DOE and NSF, United States of America. In addition, individual groups and members have received support from BCKDF, the Canada Council, Canarie, CRC, Compute Canada, FQRNT, and the Ontario Innovation Trust, Canada; EPLANET, ERC, ERDF, FP7, Horizon 2020 and Marie Skłodowska-Curie Actions, European Union; Investissements d'Avenir Labex and Idex, ANR, Région Auvergne and Fondation Partager le Savoir, France; DFG and AvH Foundation, Germany; Herakleitos, Thales and Aristeia programmes co-financed by EU-ESF and the Greek NSRF; BSF, GIF and Minerva, Israel; BRF,

Norway; CERCA Programme Generalitat de Catalunya, Generalitat Valenciana, Spain; the Royal Society and Leverhulme Trust, United Kingdom.

The crucial computing support from all WLCG partners is acknowledged gratefully, in particular from CERN, the ATLAS Tier-1 facilities at TRIUMF (Canada), NDGF (Denmark, Norway, Sweden), CC-IN2P3 (France), KIT/GridKA (Germany), INFN-CNAF (Italy), NL-T1 (Netherlands), PIC (Spain), ASGC (Taiwan), RAL (UK) and BNL (USA), the Tier-2 facilities worldwide and large non-WLCG resource providers. Major contributors of computing resources are listed in Ref. [59].

References

- [1] J. de Favereau de Jeneret, et al., High energy photon interactions at the LHC, arXiv:0908.2020 [hep-ph], 2009.
- [2] CMS Collaboration, Exclusive $\gamma\gamma \rightarrow \mu^+\mu^-$ production in proton–proton collisions at $\sqrt{s} = 7$ TeV, J. High Energy Phys. 01 (2012) 052, arXiv:1111.5536 [hep-ex].
- [3] ATLAS Collaboration, Measurement of exclusive $\gamma\gamma \rightarrow \ell^+\ell^-$ production in proton–proton collisions at $\sqrt{s} = 7$ TeV with the ATLAS detector, Phys. Lett. B 749 (2015) 242, arXiv:1506.07098 [hep-ex].
- [4] CMS Collaboration, Search for exclusive or semi-exclusive $\gamma\gamma$ production and observation of exclusive and semi-exclusive e^+e^- production in pp collisions at $\sqrt{s} = 7$ TeV, J. High Energy Phys. 11 (2012) 080, arXiv:1209.1666 [hep-ex].
- [5] CMS Collaboration, Study of exclusive two-photon production of W^+W^- in pp collisions at $\sqrt{s} = 7$ TeV and constraints on anomalous quartic gauge couplings, J. High Energy Phys. 07 (2013) 116, arXiv:1305.5596 [hep-ex].
- [6] CMS Collaboration, Evidence for exclusive $\gamma\gamma \rightarrow W^+W^-$ production and constraints on anomalous quartic gauge couplings in pp collisions at $\sqrt{s} = 7$ and 8 TeV, J. High Energy Phys. 08 (2016) 119, arXiv:1604.04464 [hep-ex].
- [7] ATLAS Collaboration, Measurement of exclusive $\gamma\gamma \rightarrow W^+W^-$ production and search for exclusive Higgs boson production in pp collisions at $\sqrt{s} = 8$ TeV using the ATLAS detector, Phys. Rev. D 94 (2016) 032011, arXiv:1607.03745 [hep-ex].
- [8] ATLAS Collaboration, Measurement of the low-mass Drell–Yan differential cross section at $\sqrt{s} = 7$ TeV using the ATLAS detector, J. High Energy Phys. 06 (2014) 112, arXiv:1404.1212 [hep-ex].
- [9] ATLAS Collaboration, Measurement of the transverse momentum and ϕ_η^* distributions of Drell–Yan lepton pairs in proton–proton collisions at $\sqrt{s} = 8$ TeV with the ATLAS detector, Eur. Phys. J. C 76 (2016) 291, arXiv:1512.02192 [hep-ex].
- [10] ATLAS Collaboration, Measurement of the double-differential high-mass Drell–Yan cross section in pp collisions at $\sqrt{s} = 8$ TeV with the ATLAS detector, J. High Energy Phys. 08 (2016) 009, arXiv:1606.01736 [hep-ex].
- [11] M. Dyndal, L. Schoeffel, The role of finite-size effects on the spectrum of equivalent photons in proton–proton collisions at the LHC, Phys. Lett. B 741 (2015) 66, arXiv:1410.2983 [hep-ph].
- [12] L.A. Harland-Lang, V.A. Khoze, M.G. Ryskin, Exclusive physics at the LHC with SuperChic 2, Eur. Phys. J. C 76 (2016) 9, arXiv:1508.02718 [hep-ph].
- [13] ATLAS Collaboration, The ATLAS experiment at the CERN large hadron collider, J. Instrum. 3 (2008) S08003.
- [14] ATLAS Collaboration, Performance of the ATLAS trigger system in 2015, Eur. Phys. J. C 77 (2017) 317, arXiv:1611.09661 [hep-ex].
- [15] M.-S. Chen, I. Muzinich, H. Terazawa, T. Cheng, Lepton pair production from two-photon processes, Phys. Rev. D 7 (1973) 3485.
- [16] V.M. Budnev, I.F. Ginzburg, G.V. Meledin, V. Serbo, The process $pp \rightarrow ppe^+e^-$ and the possibility of its calculation by means of quantum electrodynamics only, Nucl. Phys. B 63 (1973) 519.
- [17] V.M. Budnev, I.F. Ginzburg, G.V. Meledin, V.G. Serbo, The two photon particle production mechanism. Physical problems. Applications. Equivalent photon approximation, Phys. Rep. 15 (1975) 181.
- [18] M. Bähr, S. Gieseke, M. Gigg, D. Grellscheid, K. Hamilton, et al., Herwig++ physics and manual, Eur. Phys. J. C 58 (2008) 639, arXiv:0803.0883 [hep-ph].
- [19] J. Bellm, et al., Herwig 7.0/Herwig++ 3.0 release note, Eur. Phys. J. C 76 (2016) 196, arXiv:1512.01178 [hep-ph].
- [20] J.A.M. Vermaseren, Two-photon processes at very high energies, Nucl. Phys. B 229 (1983) 347.
- [21] F.W. Brasse, et al., Parametrization of the q^2 dependence of $\gamma\gamma p$ total cross sections in the resonance region, Nucl. Phys. B 110 (1976) 413.
- [22] A. Suri, D.R. Yennie, The space–time phenomenology of photon absorption and inelastic electron scattering, Ann. Phys. 72 (1972) 243.
- [23] T. Sjöstrand, High-energy physics event generation with PYTHIA 5.7 and JETSET 7.4, Comput. Phys. Commun. 82 (1994) 74.
- [24] B. Andersson, G. Gustafson, G. Ingelman, T. Sjöstrand, Parton fragmentation and string dynamics, Phys. Rep. 97 (1983) 31.

- [25] T. Sjöstrand, S. Mrenna, P.Z. Skands, A brief introduction to PYTHIA 8.1, *Comput. Phys. Commun.* 178 (2008) 852, arXiv:0710.3820 [hep-ph].
- [26] NNPDF Collaboration, R.D. Ball, et al., Parton distributions with QED corrections, *Nucl. Phys. B* 877 (2013) 290, arXiv:1308.0598 [hep-ph].
- [27] C. Schmidt, J. Pumplin, D. Stump, C.P. Yuan, CT14QED parton distribution functions from isolated photon production in deep inelastic scattering, *Phys. Rev. D* 93 (2016) 114015, arXiv:1509.02905 [hep-ph].
- [28] A.V. Manohar, P. Nason, G.P. Salam, G. Zanderighi, The photon content of the proton, *J. High Energy Phys.* 12 (2017) 046, arXiv:1708.01256 [hep-ph].
- [29] R. Corke, T. Sjöstrand, Multiparton interactions and rescattering, *J. High Energy Phys.* 01 (2010) 035, arXiv:0911.1909 [hep-ph].
- [30] P. Nason, A new method for combining NLO QCD with shower Monte Carlo algorithms, *J. High Energy Phys.* 11 (2004) 040, arXiv:hep-ph/0409146.
- [31] S. Frixione, P. Nason, C. Oleari, Matching NLO QCD computations with parton shower simulations: the POWHEG method, *J. High Energy Phys.* 11 (2007) 070, arXiv:0709.2092 [hep-ph].
- [32] S. Alioli, P. Nason, C. Oleari, E. Re, NLO vector-boson production matched with shower in POWHEG, *J. High Energy Phys.* 07 (2008) 060, arXiv:0805.4802 [hep-ph].
- [33] S. Alioli, P. Nason, C. Oleari, E. Re, A general framework for implementing NLO calculations in shower Monte Carlo programs: the POWHEG BOX, *J. High Energy Phys.* 06 (2010) 043, arXiv:1002.2581 [hep-ph].
- [34] H.-L. Lai, M. Guzzi, J. Huston, Z. Li, P.M. Nadolsky, et al., New parton distributions for collider physics, *Phys. Rev. D* 82 (2010) 074024, arXiv:1007.2241 [hep-ph].
- [35] ATLAS Collaboration, Measurement of the Z/γ^* boson transverse momentum distribution in pp collisions at $\sqrt{s} = 7$ TeV with the ATLAS detector, *J. High Energy Phys.* 09 (2014) 145, arXiv:1406.3660 [hep-ex].
- [36] J. Pumplin, D. Stump, J. Huston, H. Lai, P.M. Nadolsky, et al., New generation of parton distributions with uncertainties from global QCD analysis, *J. High Energy Phys.* 07 (2002) 012, arXiv:hep-ph/0201195.
- [37] T. Sjöstrand, S. Mrenna, P.Z. Skands, PYTHIA 6.4 physics and manual, *J. High Energy Phys.* 05 (2006) 026, arXiv:hep-ph/0603175.
- [38] P. Golonka, Z. Was, PHOTOS Monte Carlo: a precision tool for QED corrections in Z and W decays, *Eur. Phys. J. C* 45 (2006) 97, arXiv:hep-ph/0506026.
- [39] N. Davidson, T. Przedzinski, Z. Was, PHOTOS interface in C++: technical and physics documentation, *Comput. Phys. Commun.* 199 (2016) 86, arXiv:1011.0937 [hep-ph].
- [40] ATLAS Collaboration, Summary of ATLAS Pythia 8 Tunes, ATL-PHYS-PUB-2012-003, 2012, <https://cds.cern.ch/record/1474107>.
- [41] S. Agostinelli, et al., GEANT4: a simulation toolkit, *Nucl. Instrum. Methods A* 506 (2003) 250.
- [42] ATLAS Collaboration, The ATLAS simulation infrastructure, *Eur. Phys. J. C* 70 (2010) 823, arXiv:1005.4568 [physics.ins-det].
- [43] L. Frankfurt, C.E. Hyde, M. Strikman, C. Weiss, Generalized parton distributions and rapidity gap survival in exclusive diffractive pp scattering, *Phys. Rev. D* 75 (2007) 054009, arXiv:hep-ph/0608271.
- [44] M.G. Ryskin, A.D. Martin, V.A. Khoze, High-energy strong interactions: from 'hard' to 'soft', *Eur. Phys. J. C* 71 (2011) 1617, arXiv:1102.2844 [hep-ph].
- [45] ATLAS Collaboration, Muon reconstruction performance of the ATLAS detector in proton–proton collision data at $\sqrt{s} = 13$ TeV, *Eur. Phys. J. C* 76 (2016) 292, arXiv:1603.05598 [hep-ex].
- [46] C. Anastasiou, L.J. Dixon, K. Melnikov, F. Petriello, High precision QCD at hadron colliders: electroweak gauge boson rapidity distributions at next-to-next-to leading order, *Phys. Rev. D* 69 (2004) 094008, arXiv:hep-ph/0312266.
- [47] M. Czakon, A. Mitov, Top++: a program for the calculation of the top-pair cross-section at hadron colliders, *Comput. Phys. Commun.* 185 (2014) 2930, arXiv:1112.5675 [hep-ph].
- [48] ATLAS Collaboration, Measurement of distributions sensitive to the underlying event in inclusive Z -boson production in pp collisions at $\sqrt{s} = 7$ TeV with the ATLAS detector, *Eur. Phys. J. C* 74 (2014) 3195, arXiv:1409.3433 [hep-ex].
- [49] ATLAS Collaboration, Measurement of event-shape observables in $Z \rightarrow \ell^+ \ell^-$ events in pp collisions at $\sqrt{s} = 7$ TeV with the ATLAS detector at the LHC, *Eur. Phys. J. C* 76 (2016) 375, arXiv:1602.08980 [hep-ex].
- [50] CMS Collaboration, Measurement of the underlying event in the Drell–Yan process in proton–proton collisions at $\sqrt{s} = 7$ TeV, *Eur. Phys. J. C* 72 (2012) 2080, arXiv:1204.1411 [hep-ex].
- [51] ATLAS Collaboration, Measurement of W^\pm and Z -boson production cross sections in pp collisions at $\sqrt{s} = 13$ TeV with the ATLAS detector, *Phys. Lett. B* 759 (2016) 601, arXiv:1603.09222 [hep-ex].
- [52] G.G. da Silveira, L. Forthomme, K. Piotrkowski, W. Schaefer, A. Szczurek, Central $\mu^+ \mu^-$ production via photon–photon fusion in proton–proton collisions with proton dissociation, *J. High Energy Phys.* 02 (2015) 159, arXiv:1409.1541 [hep-ph].
- [53] E. Todesco, J. Wenninger, Large Hadron Collider momentum calibration and accuracy, *Phys. Rev. Accel. Beams* 20 (2017) 081003.
- [54] G. D'Agostini, A multidimensional unfolding method based on Bayes' theorem, *Nucl. Instrum. Methods A* 362 (1995) 487.
- [55] ATLAS Collaboration, Luminosity determination in pp collisions at $\sqrt{s} = 8$ TeV using the ATLAS detector at the LHC, *Eur. Phys. J. C* 76 (2016) 653, arXiv:1608.03953 [hep-ex].
- [56] A. Denner, S. Dittmaier, Production of light fermion anti-fermion pairs in gamma gamma collisions, *Eur. Phys. J. C* 9 (1999) 425, arXiv:hep-ph/9812411.
- [57] CMS and TOTEM Collaborations, CMS-TOTEM Precision Proton Spectrometer, CMS-TDR-13, TOTEM-TDR-003, 2014, <https://cds.cern.ch/record/1753795>.
- [58] ATLAS Collaboration, Technical Design Report for the ATLAS Forward Proton Detector, ATLAS-TDR-024, 2015, <https://cds.cern.ch/record/2017378>.
- [59] ATLAS Collaboration, ATLAS Computing Acknowledgements 2016–2017, ATL-GEN-PUB-2016-002, 2016, <https://cds.cern.ch/record/2202407>.

The ATLAS Collaboration

M. Aaboud^{137d}, G. Aad⁸⁸, B. Abbott¹¹⁵, O. Abdinov^{12,*}, B. Abeloos¹¹⁹, S.H. Abidi¹⁶¹, O.S. AbouZeid¹³⁹, N.L. Abraham¹⁵¹, H. Abramowicz¹⁵⁵, H. Abreu¹⁵⁴, R. Abreu¹¹⁸, Y. Abulaiti^{148a,148b}, B.S. Acharya^{167a,167b,a}, S. Adachi¹⁵⁷, L. Adamczyk^{41a}, J. Adelman¹¹⁰, M. Adersberger¹⁰², T. Adye¹³³, A.A. Affolder¹³⁹, Y. Afik¹⁵⁴, T. Agatonovic-Jovin¹⁴, C. Agheorghiesei^{28c}, J.A. Aguilar-Saavedra^{128a,128f}, S.P. Ahlen²⁴, F. Ahmadov^{68,b}, G. Aielli^{135a,135b}, S. Akatsuka⁷¹, H. Akerstedt^{148a,148b}, T.P.A. Åkesson⁸⁴, E. Akilli⁵², A.V. Akimov⁹⁸, G.L. Alberghi^{22a,22b}, J. Albert¹⁷², P. Albicocco⁵⁰, M.J. Alconada Verzini⁷⁴, S.C. Alderweireldt¹⁰⁸, M. Aleksa³², I.N. Aleksandrov⁶⁸, C. Alexa^{28b}, G. Alexander¹⁵⁵, T. Alexopoulos¹⁰, M. Alhroob¹¹⁵, B. Ali¹³⁰, M. Aliev^{76a,76b}, G. Alimonti^{94a}, J. Alison³³, S.P. Alkire³⁸, B.M.M. Allbrooke¹⁵¹, B.W. Allen¹¹⁸, P.P. Allport¹⁹, A. Aloisio^{106a,106b}, A. Alonso³⁹, F. Alonso⁷⁴, C. Alpigiani¹⁴⁰, A.A. Alshehri⁵⁶, M.I. Alstady⁸⁸, B. Alvarez Gonzalez³², D. Álvarez Piqueras¹⁷⁰, M.G. Alviggi^{106a,106b}, B.T. Amadio¹⁶, Y. Amaral Coutinho^{26a}, C. Amelung²⁵, D. Amidei⁹², S.P. Amor Dos Santos^{128a,128c}, S. Amoroso³², G. Amundsen²⁵, C. Anastopoulos¹⁴¹, L.S. Ancu⁵², N. Andari¹⁹, T. Andeen¹¹, C.F. Anders^{60b}, J.K. Anders⁷⁷, K.J. Anderson³³, A. Andreazza^{94a,94b}, V. Andrei^{60a}, S. Angelidakis³⁷, I. Angelozzi¹⁰⁹, A. Angerami³⁸, A.V. Anisenkov^{111,c}, N. Anjos¹³, A. Annovi^{126a,126b}, C. Antel^{60a}, M. Antonelli⁵⁰, A. Antonov^{100,*}, D.J. Antrim¹⁶⁶, F. Anulli^{134a}, M. Aoki⁶⁹, L. Aperio Bella³², G. Arabidze⁹³, Y. Arai⁶⁹, J.P. Araque^{128a}, V. Araujo Ferraz^{26a}, A.T.H. Arce⁴⁸, R.E. Ardell⁸⁰, F.A. Arduh⁷⁴, J-F. Arguin⁹⁷, S. Argyropoulos⁶⁶, M. Arik^{20a}, A.J. Armbruster³², L.J. Armitage⁷⁹, O. Arnaez¹⁶¹, H. Arnold⁵¹, M. Arratia³⁰, O. Arslan²³, A. Artamonov^{99,*}, G. Artoni¹²², S. Artz⁸⁶, S. Asai¹⁵⁷, N. Asbah⁴⁵, A. Ashkenazi¹⁵⁵, L. Asquith¹⁵¹, K. Assamagan²⁷, R. Astalos^{146a}, M. Atkinson¹⁶⁹, N.B. Atlaly¹⁴³,

K. Augsten¹³⁰, G. Avolio³², B. Axen¹⁶, M.K. Ayoub^{35a}, G. Azuelos^{97,d}, A.E. Baas^{60a}, M.J. Baca¹⁹, H. Bachacou¹³⁸, K. Bachas^{76a,76b}, M. Backes¹²², P. Bagnaia^{134a,134b}, M. Bahmani⁴², H. Bahrasemani¹⁴⁴, J.T. Baines¹³³, M. Bajic³⁹, O.K. Baker¹⁷⁹, P.J. Bakker¹⁰⁹, E.M. Baldin^{111,c}, P. Balek¹⁷⁵, F. Balli¹³⁸, W.K. Balunas¹²⁴, E. Banas⁴², A. Bandyopadhyay²³, Sw. Banerjee^{176,e}, A.A.E. Bannoura¹⁷⁸, L. Barak¹⁵⁵, E.L. Barberio⁹¹, D. Barberis^{53a,53b}, M. Barbero⁸⁸, T. Barillari¹⁰³, M-S Barisits³², J.T. Barkeloo¹¹⁸, T. Barklow¹⁴⁵, N. Barlow³⁰, S.L. Barnes^{36c}, B.M. Barnett¹³³, R.M. Barnett¹⁶, Z. Barnovska-Blenessy^{36a}, A. Baroncelli^{136a}, G. Barone²⁵, A.J. Barr¹²², L. Barranco Navarro¹⁷⁰, F. Barreiro⁸⁵, J. Barreiro Guimarães da Costa^{35a}, R. Bartoldus¹⁴⁵, A.E. Barton⁷⁵, P. Bartos^{146a}, A. Basalae¹²⁵, A. Bassalat^{119,f}, R.L. Bates⁵⁶, S.J. Batista¹⁶¹, J.R. Batley³⁰, M. Battaglia¹³⁹, M. Bauce^{134a,134b}, F. Bauer¹³⁸, H.S. Bawa^{145,g}, J.B. Beacham¹¹³, M.D. Beattie⁷⁵, T. Beau⁸³, P.H. Beauchemin¹⁶⁵, P. Bechtel²³, H.P. Beck^{18,h}, H.C. Beck⁵⁷, K. Becker¹²², M. Becker⁸⁶, C. Becot¹¹², A.J. Beddall^{20e}, A. Beddall^{20b}, V.A. Bednyakov⁶⁸, M. Bedognetti¹⁰⁹, C.P. Bee¹⁵⁰, T.A. Beermann³², M. Begalli^{26a}, M. Begel²⁷, J.K. Behr⁴⁵, A.S. Bell⁸¹, G. Bella¹⁵⁵, L. Bellagamba^{22a}, A. Bellerive³¹, M. Bellomo¹⁵⁴, K. Belotskiy¹⁰⁰, O. Beltramello³², N.L. Belyaev¹⁰⁰, O. Benary^{155,*}, D. Benchechroun^{137a}, M. Bender¹⁰², N. Benekos¹⁰, Y. Benhammou¹⁵⁵, E. Benhar Noccioli¹⁷⁹, J. Benitez⁶⁶, D.P. Benjamin⁴⁸, M. Benoit⁵², J.R. Bensinger²⁵, S. Bentvelsen¹⁰⁹, L. Beresford¹²², M. Beretta⁵⁰, D. Berge¹⁰⁹, E. Bergeaas Kuutmann¹⁶⁸, N. Berger⁵, J. Beringer¹⁶, S. Berlendis⁵⁸, N.R. Bernard⁸⁹, G. Bernardi⁸³, C. Bernius¹⁴⁵, F.U. Bernlochner²³, T. Berry⁸⁰, P. Berta⁸⁶, C. Bertella^{35a}, G. Bertoli^{148a,148b}, I.A. Bertram⁷⁵, C. Bertsche⁴⁵, D. Bertsche¹¹⁵, G.J. Besjes³⁹, O. Bessidskaia Bylund^{148a,148b}, M. Bessner⁴⁵, N. Besson¹³⁸, A. Bethani⁸⁷, S. Bethke¹⁰³, A.J. Bevan⁷⁹, J. Beyer¹⁰³, R.M. Bianchi¹²⁷, O. Biebel¹⁰², D. Biedermann¹⁷, R. Bielski⁸⁷, K. Bierwagen⁸⁶, N.V. Biesuz^{126a,126b}, M. Biglietti^{136a}, T.R.V. Billoud⁹⁷, H. Bilokon⁵⁰, M. Bindi⁵⁷, A. Bingul^{20b}, C. Bini^{134a,134b}, S. Biondi^{22a,22b}, T. Bisanz⁵⁷, C. Bittrich⁴⁷, D.M. Bjergaard⁴⁸, J.E. Black¹⁴⁵, K.M. Black²⁴, R.E. Blair⁶, T. Blazek^{146a}, I. Bloch⁴⁵, C. Blocker²⁵, A. Blue⁵⁶, U. Blumenschein⁷⁹, S. Blunier^{34a}, G.J. Bobbink¹⁰⁹, V.S. Bobrovnikov^{111,c}, S.S. Bocchetta⁸⁴, A. Bocci⁴⁸, C. Bock¹⁰², M. Boehler⁵¹, D. Boerner¹⁷⁸, D. Bogavac¹⁰², A.G. Bogdanchikov¹¹¹, C. Boehm^{148a}, V. Boisvert⁸⁰, P. Bokan^{168,i}, T. Bold^{41a}, A.S. Boldyrev¹⁰¹, A.E. Bolz^{60b}, M. Bomben⁸³, M. Bona⁷⁹, M. Boonekamp¹³⁸, A. Borisov¹³², G. Borissov⁷⁵, J. Bortfeldt³², D. Bortoletto¹²², V. Bortolotto^{62a,62b,62c}, D. Boscherini^{22a}, M. Bosman¹³, J.D. Bossio Sola²⁹, J. Boudreau¹²⁷, E.V. Bouhova-Thacker⁷⁵, D. Boumediene³⁷, C. Bourdarios¹¹⁹, S.K. Boutle⁵⁶, A. Boveia¹¹³, J. Boyd³², I.R. Boyko⁶⁸, A.J. Bozson⁸⁰, J. Bracinik¹⁹, A. Brandt⁸, G. Brandt⁵⁷, O. Brandt^{60a}, F. Braren⁴⁵, U. Bratzler¹⁵⁸, B. Brau⁸⁹, J.E. Brau¹¹⁸, W.D. Breaden Madden⁵⁶, K. Brendlinger⁴⁵, A.J. Brennan⁹¹, L. Brenner¹⁰⁹, R. Brenner¹⁶⁸, S. Bressler¹⁷⁵, D.L. Briglin¹⁹, T.M. Bristow⁴⁹, D. Britton⁵⁶, D. Britzger⁴⁵, F.M. Brochu³⁰, I. Brock²³, R. Brock⁹³, G. Brooijmans³⁸, T. Brooks⁸⁰, W.K. Brooks^{34b}, J. Brosamer¹⁶, E. Brost¹¹⁰, J.H. Broughton¹⁹, P.A. Bruckman de Renstrom⁴², D. Bruncko^{146b}, A. Bruni^{22a}, G. Bruni^{22a}, L.S. Bruni¹⁰⁹, S. Bruno^{135a,135b}, B.H. Brunt³⁰, M. Bruschi^{22a}, N. Bruscino¹²⁷, P. Bryant³³, L. Bryngemark⁴⁵, T. Buanes¹⁵, Q. Buat¹⁴⁴, P. Buchholz¹⁴³, A.G. Buckley⁵⁶, I.A. Budagov⁶⁸, F. Buehrer⁵¹, M.K. Bugge¹²¹, O. Bulekov¹⁰⁰, D. Bullock⁸, T.J. Burch¹¹⁰, S. Burdin⁷⁷, C.D. Burgard¹⁰⁹, A.M. Burger⁵, B. Burghgrave¹¹⁰, K. Burka⁴², S. Burke¹³³, I. Burmeister⁴⁶, J.T.P. Burr¹²², D. Büscher⁵¹, V. Büscher⁸⁶, P. Bussey⁵⁶, J.M. Butler²⁴, C.M. Buttar⁵⁶, J.M. Butterworth⁸¹, P. Butti³², W. Buttinger²⁷, A. Buzatu¹⁵³, A.R. Buzykaev^{111,c}, S. Cabrera Urbán¹⁷⁰, D. Caforio¹³⁰, H. Cai¹⁶⁹, V.M. Cairo^{40a,40b}, O. Cakir^{4a}, N. Calace⁵², P. Calafiura¹⁶, A. Calandri⁸⁸, G. Calderini⁸³, P. Calfayan⁶⁴, G. Callea^{40a,40b}, L.P. Caloba^{26a}, S. Calvente Lopez⁸⁵, D. Calvet³⁷, S. Calvet³⁷, T.P. Calvet⁸⁸, R. Camacho Toro³³, S. Camarda³², P. Camarri^{135a,135b}, D. Cameron¹²¹, R. Caminal Armadans¹⁶⁹, C. Camincher⁵⁸, S. Campana³², M. Campanelli⁸¹, A. Camplani^{94a,94b}, A. Campoverde¹⁴³, V. Canale^{106a,106b}, M. Cano Bret^{36c}, J. Cantero¹¹⁶, T. Cao¹⁵⁵, M.D.M. Capeans Garrido³², I. Caprini^{28b}, M. Caprini^{28b}, M. Capua^{40a,40b}, R.M. Carbone³⁸, R. Cardarelli^{135a}, F. Cardillo⁵¹, I. Carli¹³¹, T. Carli³², G. Carlino^{106a}, B.T. Carlson¹²⁷, L. Carminati^{94a,94b}, R.M.D. Carney^{148a,148b}, S. Caron¹⁰⁸, E. Carquin^{34b}, S. Carrá^{94a,94b}, G.D. Carrillo-Montoya³², D. Casadei¹⁹, M.P. Casado^{13,j}, M. Casolino¹³, D.W. Casper¹⁶⁶, R. Castelijns¹⁰⁹, V. Castillo Gimenez¹⁷⁰, N.F. Castro^{128a,k}, A. Catinaccio³², J.R. Catmore¹²¹, A. Cattai³², J. Caudron²³, V. Cavaliere¹⁶⁹, E. Cavallaro¹³, D. Cavalli^{94a}, M. Cavalli-Sforza¹³, V. Cavasinni^{126a,126b}, E. Celebi^{20d}, F. Ceradini^{136a,136b}, L. Cerda Alberich¹⁷⁰, A.S. Cerqueira^{26b}, A. Cerri¹⁵¹, L. Cerrito^{135a,135b}, F. Cerutti¹⁶, A. Cervelli^{22a,22b}, S.A. Cetin^{20d}, A. Chafaq^{137a}, D. Chakraborty¹¹⁰, S.K. Chan⁵⁹, W.S. Chan¹⁰⁹, Y.L. Chan^{62a}, P. Chang¹⁶⁹, J.D. Chapman³⁰, D.G. Charlton¹⁹, C.C. Chau³¹,

C.A. Chavez Barajas¹⁵¹, S. Che¹¹³, S. Cheatham^{167a,167c}, A. Chegwiddden⁹³, S. Chekanov⁶, S.V. Chekulaev^{163a}, G.A. Chelkov^{68,l}, M.A. Chelstowska³², C. Chen^{36a}, C. Chen⁶⁷, H. Chen²⁷, J. Chen^{36a}, S. Chen^{35b}, S. Chen¹⁵⁷, X. Chen^{35c,m}, Y. Chen⁷⁰, H.C. Cheng⁹², H.J. Cheng^{35a}, A. Cheplakov⁶⁸, E. Cheremushkina¹³², R. Cherkaoui El Moursli^{137e}, E. Cheu⁷, K. Cheung⁶³, L. Chevalier¹³⁸, V. Chiarella⁵⁰, G. Chiarelli^{126a,126b}, G. Chiodini^{76a}, A.S. Chisholm³², A. Chitan^{28b}, Y.H. Chiu¹⁷², M.V. Chizhov⁶⁸, K. Choi⁶⁴, A.R. Chomont³⁷, S. Chouridou¹⁵⁶, Y.S. Chow^{62a}, V. Christodoulou⁸¹, M.C. Chu^{62a}, J. Chudoba¹²⁹, A.J. Chuinard⁹⁰, J.J. Chwastowski⁴², L. Chytka¹¹⁷, A.K. Ciftci^{4a}, D. Cinca⁴⁶, V. Cindro⁷⁸, I.A. Cioara²³, A. Ciochio¹⁶, F. Ciotto^{106a,106b}, Z.H. Citron¹⁷⁵, M. Citterio^{94a}, M. Ciubancan^{28b}, A. Clark⁵², B.L. Clark⁵⁹, M.R. Clark³⁸, P.J. Clark⁴⁹, R.N. Clarke¹⁶, C. Clement^{148a,148b}, Y. Coadou⁸⁸, M. Cobal^{167a,167c}, A. Coccaro⁵², J. Cochran⁶⁷, L. Colasurdo¹⁰⁸, B. Cole³⁸, A.P. Colijn¹⁰⁹, J. Collot⁵⁸, T. Colombo¹⁶⁶, P. Conde Muiño^{128a,128b}, E. Coniavitis⁵¹, S.H. Connell^{147b}, I.A. Connelly⁸⁷, S. Constantinescu^{28b}, G. Conti³², F. Conventi^{106a,n}, M. Cooke¹⁶, A.M. Cooper-Sarkar¹²², F. Cormier¹⁷¹, K.J.R. Cormier¹⁶¹, M. Corradi^{134a,134b}, F. Corriveau^{90,o}, A. Cortes-Gonzalez³², G. Costa^{94a}, M.J. Costa¹⁷⁰, D. Costanzo¹⁴¹, G. Cottin³⁰, G. Cowan⁸⁰, B.E. Cox⁸⁷, K. Cranmer¹¹², S.J. Crawley⁵⁶, R.A. Creager¹²⁴, G. Cree³¹, S. Crépé-Renaudin⁵⁸, F. Crescioli⁸³, W.A. Cribbs^{148a,148b}, M. Cristinziani²³, V. Croft¹¹², G. Crosetti^{40a,40b}, A. Cueto⁸⁵, T. Cuhadar Donszelmann¹⁴¹, A.R. Cukierman¹⁴⁵, J. Cummings¹⁷⁹, M. Curatolo⁵⁰, J. Cúth⁸⁶, S. Czekierda⁴², P. Czodrowski³², G. D'amen^{22a,22b}, S. D'Auria⁵⁶, L. D'eraimo⁸³, M. D'Onofrio⁷⁷, M.J. Da Cunha Sargedass De Sousa^{128a,128b}, C. Da Via⁸⁷, W. Dabrowski^{41a}, T. Dado^{146a}, T. Dai⁹², O. Dale¹⁵, F. Dallaire⁹⁷, C. Dallapiccola⁸⁹, M. Dam³⁹, J.R. Dandoy¹²⁴, M.F. Daneri²⁹, N.P. Dang¹⁷⁶, A.C. Daniells¹⁹, N.S. Dann⁸⁷, M. Danninger¹⁷¹, M. Dano Hoffmann¹³⁸, V. Dao¹⁵⁰, G. Darbo^{53a}, S. Darmora⁸, J. Dassoulas³, A. Dattagupta¹¹⁸, T. Daubney⁴⁵, W. Davey²³, C. David⁴⁵, T. Davidek¹³¹, D.R. Davis⁴⁸, P. Davison⁸¹, E. Dawe⁹¹, I. Dawson¹⁴¹, K. De⁸, R. de Asmundis^{106a}, A. De Benedetti¹¹⁵, S. De Castro^{22a,22b}, S. De Cecco⁸³, N. De Groot¹⁰⁸, P. de Jong¹⁰⁹, H. De la Torre⁹³, F. De Lorenzi⁶⁷, A. De Maria⁵⁷, D. De Pedis^{134a}, A. De Salvo^{134a}, U. De Sanctis^{135a,135b}, A. De Santo¹⁵¹, K. De Vasconcelos Corga⁸⁸, J.B. De Vivie De Regie¹¹⁹, R. Debbe²⁷, C. Debenedetti¹³⁹, D.V. Dedovich⁶⁸, N. Dehghanian³, I. Deigaard¹⁰⁹, M. Del Gaudio^{40a,40b}, J. Del Peso⁸⁵, D. Delgove¹¹⁹, F. Deliot¹³⁸, C.M. Delitzsch⁷, A. Dell'Acqua³², L. Dell'Asta²⁴, M. Dell'Orso^{126a,126b}, M. Della Pietra^{106a,106b}, D. della Volpe⁵², M. Delmastro⁵, C. Delporte¹¹⁹, P.A. Delsart⁵⁸, D.A. DeMarco¹⁶¹, S. Demers¹⁷⁹, M. Demichev⁶⁸, A. Demilly⁸³, S.P. Denisov¹³², D. Denysiuk¹³⁸, D. Derendarz⁴², J.E. Derkaoui^{137d}, F. Derue⁸³, P. Dervan⁷⁷, K. Desch²³, C. Deterre⁴⁵, K. Dette¹⁶¹, M.R. Devesa²⁹, P.O. Deviveiros³², A. Dewhurst¹³³, S. Dhaliwal²⁵, F.A. Di Bello⁵², A. Di Ciaccio^{135a,135b}, L. Di Ciaccio⁵, W.K. Di Clemente¹²⁴, C. Di Donato^{106a,106b}, A. Di Girolamo³², B. Di Girolamo³², B. Di Micco^{136a,136b}, R. Di Nardo³², K.F. Di Petrillo⁵⁹, A. Di Simone⁵¹, R. Di Sipio¹⁶¹, D. Di Valentino³¹, C. Diaconu⁸⁸, M. Diamond¹⁶¹, F.A. Dias³⁹, M.A. Diaz^{34a}, E.B. Diehl⁹², J. Dietrich¹⁷, S. Díez Cornell⁴⁵, A. Dimitrievska¹⁴, J. Dingfelder²³, P. Dita^{28b}, S. Dita^{28b}, F. Dittus³², F. Djama⁸⁸, T. Djobava^{54b}, J.I. Djuvsland^{60a}, M.A.B. do Vale^{26c}, D. Dobos³², M. Dobre^{28b}, D. Dodsworth²⁵, C. Doglioni⁸⁴, J. Dolejsi¹³¹, Z. Dolezal¹³¹, M. Donadelli^{26d}, S. Donati^{126a,126b}, P. Dondero^{123a,123b}, J. Donini³⁷, J. Dopke¹³³, A. Doria^{106a}, M.T. Dova⁷⁴, A.T. Doyle⁵⁶, E. Drechsler⁵⁷, M. Dris¹⁰, Y. Du^{36b}, J. Duarte-Camperderros¹⁵⁵, F. Dubinin⁹⁸, A. Dubreuil⁵², E. Duchovni¹⁷⁵, G. Duckeck¹⁰², A. Ducourthial⁸³, O.A. Ducu^{97,p}, D. Duda¹⁰⁹, A. Dudarev³², A. Chr. Dudder⁸⁶, E.M. Duffield¹⁶, L. Duflot¹¹⁹, M. Dührssen³², C. Dulsen¹⁷⁸, M. Dumancic¹⁷⁵, A.E. Dumitriu^{28b}, A.K. Duncan⁵⁶, M. Dunford^{60a}, A. Duperrin⁸⁸, H. Duran Yildiz^{4a}, M. Düren⁵⁵, A. Durglishvili^{54b}, D. Duschinger⁴⁷, B. Dutta⁴⁵, D. Duvnjak¹, M. Dyndal⁴⁵, B.S. Dziedzic⁴², C. Eckardt⁴⁵, K.M. Ecker¹⁰³, R.C. Edgar⁹², T. Eifert³², G. Eigen¹⁵, K. Einsweiler¹⁶, T. Ekelof¹⁶⁸, M. El Kacimi^{137c}, R. El Kosseifi⁸⁸, V. Ellajosyula⁸⁸, M. Ellert¹⁶⁸, S. Elles⁵, F. Ellinghaus¹⁷⁸, A.A. Elliot¹⁷², N. Ellis³², J. Elmsheuser²⁷, M. Elsing³², D. Emeliyanov¹³³, Y. Enari¹⁵⁷, J.S. Ennis¹⁷³, M.B. Epland⁴⁸, J. Erdmann⁴⁶, A. Ereditato¹⁸, M. Ernst²⁷, S. Errede¹⁶⁹, M. Escalier¹¹⁹, C. Escobar¹⁷⁰, B. Esposito⁵⁰, O. Estrada Pastor¹⁷⁰, A.I. Etienvre¹³⁸, E. Etzion¹⁵⁵, H. Evans⁶⁴, A. Ezhilov¹²⁵, M. Ezzi^{137e}, F. Fabbri^{22a,22b}, L. Fabbri^{22a,22b}, V. Fabiani¹⁰⁸, G. Facini⁸¹, R.M. Fakhruddinov¹³², S. Falciano^{134a}, R.J. Falla⁸¹, J. Faltova³², Y. Fang^{35a}, M. Fanti^{94a,94b}, A. Farbin⁸, A. Farilla^{136a}, C. Farina¹²⁷, E.M. Farina^{123a,123b}, T. Farooque⁹³, S. Farrell¹⁶, S.M. Farrington¹⁷³, P. Farthouat³², F. Fassi^{137e}, P. Fassnacht³², D. Fassouliotis⁹, M. Faucci Giannelli⁴⁹, A. Favareto^{53a,53b}, W.J. Fawcett¹²², L. Fayard¹¹⁹, O.L. Fedin^{125,q}, W. Fedorko¹⁷¹, S. Feigl¹²¹, L. Feligioni⁸⁸, C. Feng^{36b},

E.J. Feng³², M.J. Fenton⁵⁶, A.B. Fenyuk¹³², L. Feremenga⁸, P. Fernandez Martinez¹⁷⁰, J. Ferrando⁴⁵, A. Ferrari¹⁶⁸, P. Ferrari¹⁰⁹, R. Ferrari^{123a}, D.E. Ferreira de Lima^{60b}, A. Ferrer¹⁷⁰, D. Ferrere⁵², C. Ferretti⁹², F. Fiedler⁸⁶, A. Filipčič⁷⁸, M. Filipuzzi⁴⁵, F. Filthaut¹⁰⁸, M. Fincke-Keeler¹⁷², K.D. Finelli²⁴, M.C.N. Fiolhais^{128a,128c,r}, L. Fiorini¹⁷⁰, A. Fischer², C. Fischer¹³, J. Fischer¹⁷⁸, W.C. Fisher⁹³, N. Flaschel⁴⁵, I. Fleck¹⁴³, P. Fleischmann⁹², R.R.M. Fletcher¹²⁴, T. Flick¹⁷⁸, B.M. Flierl¹⁰², L.R. Flores Castillo^{62a}, M.J. Flowerdew¹⁰³, G.T. Forcolin⁸⁷, A. Formica¹³⁸, F.A. Förster¹³, A. Forti⁸⁷, A.G. Foster¹⁹, D. Fournier¹¹⁹, H. Fox⁷⁵, S. Fracchia¹⁴¹, P. Francavilla⁸³, M. Franchini^{22a,22b}, S. Franchino^{60a}, D. Francis³², L. Franconi¹²¹, M. Franklin⁵⁹, M. Frate¹⁶⁶, M. Fraternali^{123a,123b}, D. Freeborn⁸¹, S.M. Fressard-Batraneanu³², B. Freund⁹⁷, D. Froidevaux³², J.A. Frost¹²², C. Fukunaga¹⁵⁸, T. Fusayasu¹⁰⁴, J. Fuster¹⁷⁰, O. Gabizon¹⁵⁴, A. Gabrielli^{22a,22b}, A. Gabrielli¹⁶, G.P. Gach^{41a}, S. Gadatsch³², S. Gadomski⁸⁰, G. Gagliardi^{53a,53b}, L.G. Gagnon⁹⁷, C. Galea¹⁰⁸, B. Galhardo^{128a,128c}, E.J. Gallas¹²², B.J. Gallop¹³³, P. Gallus¹³⁰, G. Galster³⁹, K.K. Gan¹¹³, S. Ganguly³⁷, Y. Gao⁷⁷, Y.S. Gao^{145,g}, F.M. Garay Walls^{34a}, C. García¹⁷⁰, J.E. García Navarro¹⁷⁰, J.A. García Pascual^{35a}, M. Garcia-Sciveres¹⁶, R.W. Gardner³³, N. Garelli¹⁴⁵, V. Garonne¹²¹, A. Gascon Bravo⁴⁵, K. Gasnikova⁴⁵, C. Gatti⁵⁰, A. Gaudiello^{53a,53b}, G. Gaudio^{123a}, I.L. Gavrilenko⁹⁸, C. Gay¹⁷¹, G. Gaycken²³, E.N. Gazis¹⁰, C.N.P. Gee¹³³, J. Geisen⁵⁷, M. Geisen⁸⁶, M.P. Geisler^{60a}, K. Gellerstedt^{148a,148b}, C. Gemme^{53a}, M.H. Genest⁵⁸, C. Geng⁹², S. Gentile^{134a,134b}, C. Gentsos¹⁵⁶, S. George⁸⁰, D. Gerbaudo¹³, G. Geßner⁴⁶, S. Ghasemi¹⁴³, M. Ghneimat²³, B. Giacobbe^{22a}, S. Giagu^{134a,134b}, N. Giangiacomi^{22a,22b}, P. Giannetti^{126a,126b}, S.M. Gibson⁸⁰, M. Gignac¹⁷¹, M. Gilchriese¹⁶, D. Gillberg³¹, G. Gilles¹⁷⁸, D.M. Gingrich^{3,d}, M.P. Giordani^{167a,167c}, F.M. Giorgi^{22a}, P.F. Giraud¹³⁸, P. Giromini⁵⁹, G. Giugliarelli^{167a,167c}, D. Giugni^{94a}, F. Giuli¹²², C. Giuliani¹⁰³, M. Giulini^{60b}, B.K. Gjelsten¹²¹, S. Gkaitatzis¹⁵⁶, I. Gkialas^{9,s}, E.L. Gkougkousis¹³, P. Gkoutoumis¹⁰, L.K. Gladilin¹⁰¹, C. Glasman⁸⁵, J. Glatzer¹³, P.C.F. Glaysheer⁴⁵, A. Glazov⁴⁵, M. Goblirsch-Kolb²⁵, J. Godlewski⁴², S. Goldfarb⁹¹, T. Golling⁵², D. Golubkov¹³², A. Gomes^{128a,128b,128d}, R. Gonçalo^{128a}, R. Goncalves Gama^{26a}, J. Goncalves Pinto Firmino Da Costa¹³⁸, G. Gonella⁵¹, L. Gonella¹⁹, A. Gongadze⁶⁸, J.L. Gonski⁵⁹, S. González de la Hoz¹⁷⁰, S. Gonzalez-Sevilla⁵², L. Goossens³², P.A. Gorbounov⁹⁹, H.A. Gordon²⁷, I. Gorelov¹⁰⁷, B. Gorini³², E. Gorini^{76a,76b}, A. Gorišek⁷⁸, A.T. Goshaw⁴⁸, C. Gössling⁴⁶, M.I. Gostkin⁶⁸, C.A. Gottardo²³, C.R. Goudet¹¹⁹, D. Goujdami^{137c}, A.G. Goussiou¹⁴⁰, N. Govender^{147b,t}, E. Gozani¹⁵⁴, I. Grabowska-Bold^{41a}, P.O.J. Gradin¹⁶⁸, J. Gramling¹⁶⁶, E. Gramstad¹²¹, S. Grancagnolo¹⁷, V. Gratchev¹²⁵, P.M. Gravila^{28f}, C. Gray⁵⁶, H.M. Gray¹⁶, Z.D. Greenwood^{82,u}, C. Grefe²³, K. Gregersen⁸¹, I.M. Gregor⁴⁵, P. Grenier¹⁴⁵, K. Grevtsov⁵, J. Griffiths⁸, A.A. Grillo¹³⁹, K. Grimm⁷⁵, S. Grinstein^{13,v}, Ph. Gris³⁷, J.-F. Grivaz¹¹⁹, S. Groh⁸⁶, E. Gross¹⁷⁵, J. Grosse-Knetter⁵⁷, G.C. Grossi⁸², Z.J. Grout⁸¹, A. Grummer¹⁰⁷, L. Guan⁹², W. Guan¹⁷⁶, J. Guenther³², F. Guescini^{163a}, D. Guest¹⁶⁶, O. Gueta¹⁵⁵, B. Gui¹¹³, E. Guido^{53a,53b}, T. Guillemain⁵, S. Guindon³², U. Gul⁵⁶, C. Gumpert³², J. Guo^{36c}, W. Guo⁹², Y. Guo^{36a}, R. Gupta⁴³, S. Gurbuz^{20a}, G. Gustavino¹¹⁵, B.J. Gutelman¹⁵⁴, P. Gutierrez¹¹⁵, N.G. Gutierrez Ortiz⁸¹, C. Gutsche⁸¹, C. Guyot¹³⁸, M.P. Guzik^{41a}, C. Gwenlan¹²², C.B. Gwilliam⁷⁷, A. Haas¹¹², C. Haber¹⁶, H.K. Hadavand⁸, N. Haddad^{137e}, A. Hadeef⁸⁸, S. Hageböck²³, M. Hagihara¹⁶⁴, H. Hakobyan^{180,*}, M. Haleem⁴⁵, J. Haley¹¹⁶, G. Halladjian⁹³, G.D. Hallowell⁸⁸, K. Hamacher¹⁷⁸, P. Hamal¹¹⁷, K. Hamano¹⁷², A. Hamilton^{147a}, G.N. Hamity¹⁴¹, P.G. Hamnett⁴⁵, L. Han^{36a}, S. Han^{35a}, K. Hanagaki^{69,w}, K. Hanawa¹⁵⁷, M. Hance¹³⁹, D.M. Handl¹⁰², B. Haney¹²⁴, P. Hanke^{60a}, J.B. Hansen³⁹, J.D. Hansen³⁹, M.C. Hansen²³, P.H. Hansen³⁹, K. Hara¹⁶⁴, A.S. Hard¹⁷⁶, T. Harenberg¹⁷⁸, F. Hariri¹¹⁹, S. Harkusha⁹⁵, P.F. Harrison¹⁷³, N.M. Hartmann¹⁰², Y. Hasegawa¹⁴², A. Hasib⁴⁹, S. Hassani¹³⁸, S. Haug¹⁸, R. Hauser⁹³, L. Hauswald⁴⁷, L.B. Havener³⁸, M. Havranek¹³⁰, C.M. Hawkes¹⁹, R.J. Hawking³², D. Hayakawa¹⁵⁹, D. Hayden⁹³, C.P. Hays¹²², J.M. Hays⁷⁹, H.S. Hayward⁷⁷, S.J. Haywood¹³³, S.J. Head¹⁹, T. Heck⁸⁶, V. Hedberg⁸⁴, L. Heelan⁸, S. Heer²³, K.K. Heidegger⁵¹, S. Heim⁴⁵, T. Heim¹⁶, B. Heinemann^{45,x}, J.J. Heinrich¹⁰², L. Heinrich¹¹², C. Heinz⁵⁵, J. Hejbal¹²⁹, L. Helary³², A. Held¹⁷¹, S. Hellman^{148a,148b}, C. Helsens³², R.C.W. Henderson⁷⁵, Y. Heng¹⁷⁶, S. Henkelmann¹⁷¹, A.M. Henriques Correia³², S. Henrot-Versille¹¹⁹, G.H. Herbert¹⁷, H. Herde²⁵, V. Herget¹⁷⁷, Y. Hernández Jiménez^{147c}, H. Herr⁸⁶, G. Herten⁵¹, R. Hertenberger¹⁰², L. Hervas³², T.C. Herwig¹²⁴, G.G. Hesketh⁸¹, N.P. Hessey^{163a}, J.W. Hetherly⁴³, S. Higashino⁶⁹, E. Higón-Rodríguez¹⁷⁰, K. Hildebrand³³, E. Hill¹⁷², J.C. Hill³⁰, K.H. Hiller⁴⁵, S.J. Hillier¹⁹, M. Hils⁴⁷, I. Hinchliffe¹⁶, M. Hirose⁵¹, D. Hirschbuehl¹⁷⁸, B. Hiti⁷⁸, O. Hladik¹²⁹, D.R. Hlaluku^{147c}, X. Hoad⁴⁹, J. Hobbs¹⁵⁰, N. Hod^{163a}, M.C. Hodgkinson¹⁴¹, P. Hodgson¹⁴¹,

A. Hoecker³², M.R. Hoferkamp¹⁰⁷, F. Hoenig¹⁰², D. Hohn²³, T.R. Holmes³³, M. Homann⁴⁶, S. Honda¹⁶⁴, T. Honda⁶⁹, T.M. Hong¹²⁷, B.H. Hooberman¹⁶⁹, W.H. Hopkins¹¹⁸, Y. Horii¹⁰⁵, A.J. Horton¹⁴⁴, J.-Y. Hostachy⁵⁸, A. Hostiuc¹⁴⁰, S. Hou¹⁵³, A. Hoummada^{137a}, J. Howarth⁸⁷, J. Hoya⁷⁴, M. Hrabovsky¹¹⁷, J. Hrdinka³², I. Hristova¹⁷, J. Hrivnac¹¹⁹, T. Hryn'ova⁵, A. Hrynevich⁹⁶, P.J. Hsu⁶³, S.-C. Hsu¹⁴⁰, Q. Hu²⁷, S. Hu^{36c}, Y. Huang^{35a}, Z. Hubacek¹³⁰, F. Hubaut⁸⁸, F. Huegging²³, T.B. Huffman¹²², E.W. Hughes³⁸, M. Huhtinen³², R.F.H. Hunter³¹, P. Huo¹⁵⁰, N. Huseynov^{68,b}, J. Huston⁹³, J. Huth⁵⁹, R. Hyneman⁹², G. Iacobucci⁵², G. Iakovidis²⁷, I. Ibragimov¹⁴³, L. Iconomidou-Fayard¹¹⁹, Z. Idrissi^{137e}, P. Iengo³², O. Igonkina^{109,y}, T. Iizawa¹⁷⁴, Y. Ikegami⁶⁹, M. Ikeno⁶⁹, Y. Ilchenko^{11,z}, D. Iliadis¹⁵⁶, N. Ilic¹⁴⁵, F. Iltzsche⁴⁷, G. Introzzi^{123a,123b}, P. Ioannou^{9,*}, M. Iodice^{136a}, K. Iordanidou³⁸, V. Ippolito⁵⁹, M.F. Isacson¹⁶⁸, N. Ishijima¹²⁰, M. Ishino¹⁵⁷, M. Ishitsuka¹⁵⁹, C. Issever¹²², S. Istin^{20a}, F. Ito¹⁶⁴, J.M. Iturbe Ponce^{62a}, R. Iuppa^{162a,162b}, H. Iwasaki⁶⁹, J.M. Izen⁴⁴, V. Izzo^{106a}, S. Jabbar³, P. Jackson¹, R.M. Jacobs²³, V. Jain², K.B. Jakobi⁸⁶, K. Jakobs⁵¹, S. Jakobsen⁶⁵, T. Jakoubek¹²⁹, D.O. Jamin¹¹⁶, D.K. Jana⁸², R. Jansky⁵², J. Janssen²³, M. Janus⁵⁷, P.A. Janus^{41a}, G. Jarlskog⁸⁴, N. Javadov^{68,b}, T. Javůrek⁵¹, M. Javurkova⁵¹, F. Jeanneau¹³⁸, L. Jeanty¹⁶, J. Jejelava^{54a,aa}, A. Jelinskas¹⁷³, P. Jenni^{51,ab}, C. Jeske¹⁷³, S. Jézéquel⁵, H. Ji¹⁷⁶, J. Jia¹⁵⁰, H. Jiang⁶⁷, Y. Jiang^{36a}, Z. Jiang¹⁴⁵, S. Jiggins⁸¹, J. Jimenez Pena¹⁷⁰, S. Jin^{35b}, A. Jinaru^{28b}, O. Jinnouchi¹⁵⁹, H. Jivan^{147c}, P. Johansson¹⁴¹, K.A. Johns⁷, C.A. Johnson⁶⁴, W.J. Johnson¹⁴⁰, K. Jon-And^{148a,148b}, R.W.L. Jones⁷⁵, S.D. Jones¹⁵¹, S. Jones⁷, T.J. Jones⁷⁷, J. Jongmanns^{60a}, P.M. Jorge^{128a,128b}, J. Jovicevic^{163a}, X. Ju¹⁷⁶, A. Juste Rozas^{13,v}, M.K. Köhler¹⁷⁵, A. Kaczmarska⁴², M. Kado¹¹⁹, H. Kagan¹¹³, M. Kagan¹⁴⁵, S.J. Kahn⁸⁸, T. Kaji¹⁷⁴, E. Kajomovitz¹⁵⁴, C.W. Kalderon⁸⁴, A. Kaluza⁸⁶, S. Kama⁴³, A. Kamenshchikov¹³², N. Kanaya¹⁵⁷, L. Kanjir⁷⁸, V.A. Kantserov¹⁰⁰, J. Kanzaki⁶⁹, B. Kaplan¹¹², L.S. Kaplan¹⁷⁶, D. Kar^{147c}, K. Karakostas¹⁰, N. Karastathis¹⁰, M.J. Kareem^{163b}, E. Karentzos¹⁰, S.N. Karpov⁶⁸, Z.M. Karpova⁶⁸, K. Karthik¹¹², V. Kartvelishvili⁷⁵, A.N. Karyukhin¹³², K. Kasahara¹⁶⁴, L. Kashif¹⁷⁶, R.D. Kass¹¹³, A. Kastanas¹⁴⁹, Y. Kataoka¹⁵⁷, C. Kato¹⁵⁷, A. Katre⁵², J. Katzy⁴⁵, K. Kawade⁷⁰, K. Kawagoe⁷³, T. Kawamoto¹⁵⁷, G. Kawamura⁵⁷, E.F. Kay⁷⁷, V.F. Kazanin^{111,c}, R. Keeler¹⁷², R. Kehoe⁴³, J.S. Keller³¹, E. Kellermann⁸⁴, J.J. Kempster⁸⁰, J. Kendrick¹⁹, H. Keoshkerian¹⁶¹, O. Kepka¹²⁹, B.P. Kerševan⁷⁸, S. Kersten¹⁷⁸, R.A. Keyes⁹⁰, M. Khader¹⁶⁹, F. Khalil-zada¹², A. Khanov¹¹⁶, A.G. Kharlamov^{111,c}, T. Kharlamova^{111,c}, A. Khodinov¹⁶⁰, T.J. Khoo⁵², V. Khovanskiy^{99,*}, E. Khramov⁶⁸, J. Khubua^{54b,ac}, S. Kido⁷⁰, C.R. Kilby⁸⁰, H.Y. Kim⁸, S.H. Kim¹⁶⁴, Y.K. Kim³³, N. Kimura¹⁵⁶, O.M. Kind¹⁷, B.T. King⁷⁷, D. Kirchmeier⁴⁷, J. Kirk¹³³, A.E. Kiryunin¹⁰³, T. Kishimoto¹⁵⁷, D. Kisielewska^{41a}, V. Kitali⁴⁵, O. Kivernyk⁵, E. Kladiva^{146b}, T. Klapdor-Kleingrothaus⁵¹, M.H. Klein⁹², M. Klein⁷⁷, U. Klein⁷⁷, K. Kleinknecht⁸⁶, P. Klimek¹¹⁰, A. Klimentov²⁷, R. Klingenberg^{46,*}, T. Klingl²³, T. Klioutchnikova³², F.F. Klitzner¹⁰², E.-E. Kluge^{60a}, P. Kluit¹⁰⁹, S. Kluth¹⁰³, E. Kneringer⁶⁵, E.B.F.G. Knoops⁸⁸, A. Knue¹⁰³, A. Kobayashi¹⁵⁷, D. Kobayashi⁷³, T. Kobayashi¹⁵⁷, M. Kobel⁴⁷, M. Kocian¹⁴⁵, P. Kodys¹³¹, T. Koffas³¹, E. Koffeman¹⁰⁹, N.M. Köhler¹⁰³, T. Koi¹⁴⁵, M. Kolb^{60b}, I. Koletsou⁵, A.A. Komar^{98,*}, T. Kondo⁶⁹, N. Kondrashova^{36c}, K. Köneke⁵¹, A.C. König¹⁰⁸, T. Kono^{69,ad}, R. Konoplich^{112,ae}, N. Konstantinidis⁸¹, B. Konya⁸⁴, R. Kopeliansky⁶⁴, S. Koperny^{41a}, A.K. Kopp⁵¹, K. Korcyl⁴², K. Kordas¹⁵⁶, A. Korn⁸¹, A.A. Korol^{111,c}, I. Korolkov¹³, E.V. Korolkova¹⁴¹, O. Kortner¹⁰³, S. Kortner¹⁰³, T. Kosek¹³¹, V.V. Kostyukhin²³, A. Kotwal⁴⁸, A. Koulouris¹⁰, A. Kourkoulis-Charalampidi^{123a,123b}, C. Kourkoulis⁹, E. Kourlitis¹⁴¹, V. Kouskoura²⁷, A.B. Kowalewska⁴², R. Kowalewski¹⁷², T.Z. Kowalski^{41a}, C. Kozakai¹⁵⁷, W. Kozanecki¹³⁸, A.S. Kozhin¹³², V.A. Kramarenko¹⁰¹, G. Kramberger⁷⁸, D. Krasnopevtsev¹⁰⁰, M.W. Krasny⁸³, A. Krasznahorkay³², D. Krauss¹⁰³, J.A. Kremer^{41a}, J. Kretschmar⁷⁷, K. Kreutzfeldt⁵⁵, P. Krieger¹⁶¹, K. Krizka¹⁶, K. Kroeninger⁴⁶, H. Kroha¹⁰³, J. Kroll¹²⁹, J. Kroll¹²⁴, J. Kroseberg²³, J. Krstic¹⁴, U. Kruchonak⁶⁸, H. Krüger²³, N. Krumnack⁶⁷, M.C. Kruse⁴⁸, T. Kubota⁹¹, H. Kucuk⁸¹, S. Kuday^{4b}, J.T. Kuechler¹⁷⁸, S. Kuehn³², A. Kugel^{60a}, F. Kuger¹⁷⁷, T. Kuhl⁴⁵, V. Kukhtin⁶⁸, R. Kukla⁸⁸, Y. Kulchitsky⁹⁵, S. Kuleshov^{34b}, Y.P. Kulinich¹⁶⁹, M. Kuna^{134a,134b}, T. Kunigo⁷¹, A. Kupco¹²⁹, T. Kupfer⁴⁶, O. Kuprash¹⁵⁵, H. Kurashige⁷⁰, L.L. Kurchaninov^{163a}, Y.A. Kurochkin⁹⁵, M.G. Kurth^{35a}, E.S. Kuwertz¹⁷², M. Kuze¹⁵⁹, J. Kvita¹¹⁷, T. Kwan¹⁷², D. Kyriazopoulos¹⁴¹, A. La Rosa¹⁰³, J.L. La Rosa Navarro^{26d}, L. La Rotonda^{40a,40b}, F. La Ruffa^{40a,40b}, C. Lacasta¹⁷⁰, F. Lacava^{134a,134b}, J. Lacey⁴⁵, D.P.J. Lack⁸⁷, H. Lacker¹⁷, D. Lacour⁸³, E. Ladygin⁶⁸, R. Lafaye⁵, B. Laforge⁸³, T. Lagouri¹⁷⁹, S. Lai⁵⁷, S. Lammers⁶⁴, W. Lampl⁷, E. Lançon²⁷, U. Landgraf⁵¹, M.P.J. Landon⁷⁹, M.C. Lanfermann⁵², V.S. Lang⁴⁵, J.C. Lange¹³, R.J. Langenberg³², A.J. Lankford¹⁶⁶, F. Lanni²⁷, K. Lantzsch²³, A. Lanza^{123a}, A. Lapertosa^{53a,53b}, S. Laplace⁸³, J.F. Laporte¹³⁸,

T. Lari^{94a}, F. Lasagni Manghi^{22a,22b}, M. Lassnig³², T.S. Lau^{62a}, P. Laurelli⁵⁰, W. Lavrijsen¹⁶, A.T. Law¹³⁹, P. Laycock⁷⁷, T. Lazovich⁵⁹, M. Lazzaroni^{94a,94b}, B. Le⁹¹, O. Le Dortz⁸³, E. Le Guirriec⁸⁸, E.P. Le Quilleuc¹³⁸, M. LeBlanc¹⁷², T. LeCompte⁶, F. Ledroit-Guillon⁵⁸, C.A. Lee²⁷, G.R. Lee^{34a}, S.C. Lee¹⁵³, L. Lee⁵⁹, B. Lefebvre⁹⁰, G. Lefebvre⁸³, M. Lefebvre¹⁷², F. Legger¹⁰², C. Leggett¹⁶, G. Lehmann Miotto³², X. Lei⁷, W.A. Leight⁴⁵, M.A.L. Leite^{26d}, R. Leitner¹³¹, D. Lellouch¹⁷⁵, B. Lemmer⁵⁷, K.J.C. Leney⁸¹, T. Lenz²³, B. Lenzi³², R. Leone⁷, S. Leone^{126a,126b}, C. Leonidopoulos⁴⁹, G. Lerner¹⁵¹, C. Leroy⁹⁷, R. Les¹⁶¹, A.A.J. Lesage¹³⁸, C.G. Lester³⁰, M. Levchenko¹²⁵, J. Levêque⁵, D. Levin⁹², L.J. Levinson¹⁷⁵, M. Levy¹⁹, D. Lewis⁷⁹, B. Li^{36a,af}, Changqiao Li^{36a}, H. Li¹⁵⁰, L. Li^{36c}, Q. Li^{35a}, Q. Li^{36a}, S. Li⁴⁸, X. Li^{36c}, Y. Li¹⁴³, Z. Liang^{35a}, B. Liberti^{135a}, A. Liblong¹⁶¹, K. Lie^{62c}, J. Liebal²³, W. Liebig¹⁵, A. Limosani¹⁵², K. Lin⁹³, S.C. Lin¹⁸², T.H. Lin⁸⁶, R.A. Linck⁶⁴, B.E. Lindquist¹⁵⁰, A.E. Lioni⁵², E. Lipeles¹²⁴, A. Lipniacka¹⁵, M. Lisovsky^{60b}, T.M. Liss^{169,ag}, A. Lister¹⁷¹, A.M. Litke¹³⁹, B. Liu⁶⁷, H. Liu⁹², H. Liu²⁷, J.K.K. Liu¹²², J. Liu^{36b}, J.B. Liu^{36a}, K. Liu⁸⁸, L. Liu¹⁶⁹, M. Liu^{36a}, Y.L. Liu^{36a}, Y. Liu^{36a}, M. Livan^{123a,123b}, A. Lleres⁵⁸, J. Llorente Merino^{35a}, S.L. Lloyd⁷⁹, C.Y. Lo^{62b}, F. Lo Sterzo⁴³, E.M. Lobodzinska⁴⁵, P. Loch⁷, F.K. Loebinger⁸⁷, A. Loesle⁵¹, K.M. Loew²⁵, T. Lohse¹⁷, K. Lohwasser¹⁴¹, M. Lokajicek¹²⁹, B.A. Long²⁴, J.D. Long¹⁶⁹, R.E. Long⁷⁵, L. Longo^{76a,76b}, K.A. Looper¹¹³, J.A. Lopez^{34b}, I. Lopez Paz¹³, A. Lopez Solis⁸³, J. Lorenz¹⁰², N. Lorenzo Martinez⁵, M. Losada²¹, P.J. Lösel¹⁰², X. Lou^{35a}, A. Lounis¹¹⁹, J. Love⁶, P.A. Love⁷⁵, H. Lu^{62a}, N. Lu⁹², Y.J. Lu⁶³, H.J. Lubatti¹⁴⁰, C. Luci^{134a,134b}, A. Lucotte⁵⁸, C. Luedtke⁵¹, F. Luehring⁶⁴, W. Lukas⁶⁵, L. Luminari^{134a}, O. Lundberg^{148a,148b}, B. Lund-Jensen¹⁴⁹, M.S. Lutz⁸⁹, P.M. Luzi⁸³, D. Lynn²⁷, R. Lysak¹²⁹, E. Lytken⁸⁴, F. Lyu^{35a}, V. Lyubushkin⁶⁸, H. Ma²⁷, L.L. Ma^{36b}, Y. Ma^{36b}, G. Maccarrone⁵⁰, A. Macchiolo¹⁰³, C.M. Macdonald¹⁴¹, B. Maček⁷⁸, J. Machado Miguens^{124,128b}, D. Madaffari¹⁷⁰, R. Madar³⁷, W.F. Mader⁴⁷, A. Madsen⁴⁵, N. Madysa⁴⁷, J. Maeda⁷⁰, S. Maeland¹⁵, T. Maeno²⁷, A.S. Maevskiy¹⁰¹, V. Magerl⁵¹, C. Maiani¹¹⁹, C. Maidantchik^{26a}, T. Maier¹⁰², A. Maio^{128a,128b,128d}, O. Majersky^{146a}, S. Majewski¹¹⁸, Y. Makida⁶⁹, N. Makovec¹¹⁹, B. Malaescu⁸³, Pa. Malecki⁴², V.P. Maleev¹²⁵, F. Malek⁵⁸, U. Mallik⁶⁶, D. Malon⁶, C. Malone³⁰, S. Maltezos¹⁰, S. Malyukov³², J. Mamuzic¹⁷⁰, G. Mancini⁵⁰, I. Mandić⁷⁸, J. Maneira^{128a,128b}, L. Manhaes de Andrade Filho^{26b}, J. Manjarres Ramos⁴⁷, K.H. Mankinen⁸⁴, A. Mann¹⁰², A. Manousos³², B. Mansoulie¹³⁸, J.D. Mansour^{35a}, R. Mantifel⁹⁰, M. Mantoani⁵⁷, S. Manzoni^{94a,94b}, L. Mapelli³², G. Marceca²⁹, L. March⁵², L. Marchese¹²², G. Marchiori⁸³, M. Marcisovsky¹²⁹, C.A. Marin Tobon³², M. Marjanovic³⁷, D.E. Marley⁹², F. Marroquim^{26a}, S.P. Marsden⁸⁷, Z. Marshall¹⁶, M.U.F. Martensson¹⁶⁸, S. Marti-Garcia¹⁷⁰, C.B. Martin¹¹³, T.A. Martin¹⁷³, V.J. Martin⁴⁹, B. Martin dit Latour¹⁵, M. Martinez^{13,v}, V.I. Martinez Outschoorn¹⁶⁹, S. Martin-Haugh¹³³, V.S. Martoiu^{28b}, A.C. Martyniuk⁸¹, A. Marzin³², L. Masetti⁸⁶, T. Mashimo¹⁵⁷, R. Mashinistov⁹⁸, J. Masik⁸⁷, A.L. Maslennikov^{111,c}, L.H. Mason⁹¹, L. Massa^{135a,135b}, P. Mastrandrea⁵, A. Mastroberardino^{40a,40b}, T. Masubuchi¹⁵⁷, P. Mättig¹⁷⁸, J. Maurer^{28b}, S.J. Maxfield⁷⁷, D.A. Maximov^{111,c}, R. Mazini¹⁵³, I. Maznas¹⁵⁶, S.M. Mazza^{94a,94b}, N.C. Mc Fadden¹⁰⁷, G. Mc Goldrick¹⁶¹, S.P. Mc Kee⁹², A. McCarn⁹², R.L. McCarthy¹⁵⁰, T.G. McCarthy¹⁰³, L.I. McClymont⁸¹, E.F. McDonald⁹¹, J.A. Mcfayden³², G. Mchedlidze⁵⁷, S.J. McMahon¹³³, P.C. McNamara⁹¹, C.J. McNicol¹⁷³, R.A. McPherson^{172,o}, S. Meehan¹⁴⁰, T.J. Megy⁵¹, S. Mehlhase¹⁰², A. Mehta⁷⁷, T. Meideck⁵⁸, K. Meier^{60a}, B. Meirose⁴⁴, D. Melini^{170,ah}, B.R. Mellado Garcia^{147c}, J.D. Mellenthin⁵⁷, M. Melo^{146a}, F. Meloni¹⁸, A. Melzer²³, S.B. Menary⁸⁷, L. Meng⁷⁷, X.T. Meng⁹², A. Mengarelli^{22a,22b}, S. Menke¹⁰³, E. Meoni^{40a,40b}, S. Mergelmeyer¹⁷, C. Merlassino¹⁸, P. Mermod⁵², L. Merola^{106a,106b}, C. Meroni^{94a}, F.S. Merritt³³, A. Messina^{134a,134b}, J. Metcalfe⁶, A.S. Mete¹⁶⁶, C. Meyer¹²⁴, J.-P. Meyer¹³⁸, J. Meyer¹⁰⁹, H. Meyer Zu Theenhausen^{60a}, F. Miano¹⁵¹, R.P. Middleton¹³³, S. Miglioranzi^{53a,53b}, L. Mijović⁴⁹, G. Mikenberg¹⁷⁵, M. Mikestikova¹²⁹, M. Mikuž⁷⁸, M. Milesi⁹¹, A. Milic¹⁶¹, D.A. Millar⁷⁹, D.W. Miller³³, C. Mills⁴⁹, A. Milov¹⁷⁵, D.A. Milstead^{148a,148b}, A.A. Minaenko¹³², Y. Minami¹⁵⁷, I.A. Minashvili^{54b}, A.I. Mincer¹¹², B. Mindur^{41a}, M. Mineev⁶⁸, Y. Minegishi¹⁵⁷, Y. Ming¹⁷⁶, L.M. Mir¹³, A. Mirto^{76a,76b}, K.P. Mistry¹²⁴, T. Mitani¹⁷⁴, J. Mitrevski¹⁰², V.A. Mitsou¹⁷⁰, A. Miucci¹⁸, P.S. Miyagawa¹⁴¹, A. Mizukami⁶⁹, J.U. Mjörnmark⁸⁴, T. Mkrtchyan¹⁸⁰, M. Mlynarikova¹³¹, T. Moa^{148a,148b}, K. Mochizuki⁹⁷, P. Mogg⁵¹, S. Mohapatra³⁸, S. Molander^{148a,148b}, R. Moles-Valls²³, M.C. Mondragon⁹³, K. Mönig⁴⁵, J. Monk³⁹, E. Monnier⁸⁸, A. Montalbano¹⁵⁰, J. Montejo Berlingen³², F. Monticelli⁷⁴, S. Monzani^{94a,94b}, R.W. Moore³, N. Morange¹¹⁹, D. Moreno²¹, M. Moreno Llacer³², P. Morettini^{53a}, S. Morgenstern³², D. Mori¹⁴⁴, T. Mori¹⁵⁷, M. Morii⁵⁹, M. Morinaga¹⁷⁴, V. Morisbak¹²¹, A.K. Morley³², G. Mornacchi³²,

J.D. Morris⁷⁹, L. Morvaj¹⁵⁰, P. Moschovakos¹⁰, M. Mosidze^{54b}, H.J. Moss¹⁴¹, J. Moss^{145,ai}, K. Motohashi¹⁵⁹, R. Mount¹⁴⁵, E. Mountricha²⁷, E.J.W. Moyse⁸⁹, S. Muanza⁸⁸, F. Mueller¹⁰³, J. Mueller¹²⁷, R.S.P. Mueller¹⁰², D. Muenstermann⁷⁵, P. Mullen⁵⁶, G.A. Mullier¹⁸, F.J. Munoz Sanchez⁸⁷, W.J. Murray^{173,133}, H. Musheghyan³², M. Muškinja⁷⁸, A.G. Myagkov^{132,aj}, M. Myska¹³⁰, B.P. Nachman¹⁶, O. Nackenhorst⁵², K. Nagai¹²², R. Nagai^{69,ad}, K. Nagano⁶⁹, Y. Nagasaka⁶¹, K. Nagata¹⁶⁴, M. Nagel⁵¹, E. Nagy⁸⁸, A.M. Nairz³², Y. Nakahama¹⁰⁵, K. Nakamura⁶⁹, T. Nakamura¹⁵⁷, I. Nakano¹¹⁴, R.F. Naranjo Garcia⁴⁵, R. Narayan¹¹, D.I. Narrias Villar^{60a}, I. Naryshkin¹²⁵, T. Naumann⁴⁵, G. Navarro²¹, R. Nayyar⁷, H.A. Neal⁹², P.Yu. Nechaeva⁹⁸, T.J. Neep¹³⁸, A. Negri^{123a,123b}, M. Negrini^{22a}, S. Nektarijevic¹⁰⁸, C. Nellist⁵⁷, A. Nelson¹⁶⁶, M.E. Nelson¹²², S. Nemecek¹²⁹, P. Nemethy¹¹², M. Nessi^{32,ak}, M.S. Neubauer¹⁶⁹, M. Neumann¹⁷⁸, P.R. Newman¹⁹, T.Y. Ng^{62c}, T. Nguyen Manh⁹⁷, R.B. Nickerson¹²², R. Nicolaïdou¹³⁸, J. Nielsen¹³⁹, N. Nikiforou¹¹, V. Nikolaenko^{132,aj}, I. Nikolic-Audit⁸³, K. Nikolopoulos¹⁹, J.K. Nilsen¹²¹, P. Nilsson²⁷, Y. Ninomiya⁶⁹, A. Nisati^{134a}, N. Nishu^{36c}, R. Nisius¹⁰³, I. Nitsche⁴⁶, T. Nitta¹⁷⁴, T. Nobe¹⁵⁷, Y. Noguchi⁷¹, M. Nomachi¹²⁰, I. Nomidis³¹, M.A. Nomura²⁷, T. Nooney⁷⁹, M. Nordberg³², N. Norjoharuddeen¹²², O. Novgorodova⁴⁷, M. Nozaki⁶⁹, L. Nozka¹¹⁷, K. Ntekas¹⁶⁶, E. Nurse⁸¹, F. Nuti⁹¹, K. O'Connor²⁵, D.C. O'Neil¹⁴⁴, A.A. O'Rourke⁴⁵, V. O'Shea⁵⁶, F.G. Oakham^{31,d}, H. Oberlack¹⁰³, T. Obermann²³, J. Ocariz⁸³, A. Ochi⁷⁰, I. Ochoa³⁸, J.P. Ochoa-Ricoux^{34a}, S. Oda⁷³, S. Odaka⁶⁹, A. Oh⁸⁷, S.H. Oh⁴⁸, C.C. Ohm¹⁴⁹, H. Ohman¹⁶⁸, H. Oide^{53a,53b}, H. Okawa¹⁶⁴, Y. Okumura¹⁵⁷, T. Okuyama⁶⁹, A. Olariu^{28b}, L.F. Oleiro Seabra^{128a}, S.A. Olivares Pino^{34a}, D. Oliveira Damazio²⁷, A. Olszewski⁴², J. Olszowska⁴², A. Onofre^{128a,128e}, K. Onogi¹⁰⁵, P.U.E. Onyisi^{11,z}, H. Oppen¹²¹, M.J. Oreglia³³, Y. Oren¹⁵⁵, D. Orestano^{136a,136b}, N. Orlando^{62b}, R.S. Orr¹⁶¹, B. Osculati^{53a,53b,*}, R. Ospanov^{36a}, G. Otero y Garzon²⁹, H. Otono⁷³, M. Ouchrif^{137d}, F. Ould-Saada¹²¹, A. Ouraou¹³⁸, K.P. Oussoren¹⁰⁹, Q. Ouyang^{35a}, M. Owen⁵⁶, R.E. Owen¹⁹, V.E. Ozcan^{20a}, N. Ozturk⁸, K. Pachal¹⁴⁴, A. Pacheco Pages¹³, L. Pacheco Rodriguez¹³⁸, C. Padilla Aranda¹³, S. Pagan Griso¹⁶, M. Paganini¹⁷⁹, F. Paige²⁷, G. Palacino⁶⁴, S. Palazzo^{40a,40b}, S. Palestini³², M. Palka^{41b}, D. Pallin³⁷, E. St. Panagiotopoulou¹⁰, I. Panagoulas¹⁰, C.E. Pandini⁵², J.G. Panduro Vazquez⁸⁰, P. Pani³², S. Panitkin²⁷, D. Pantea^{28b}, L. Paolozzi⁵², Th.D. Papadopoulos¹⁰, K. Papageorgiou^{9,s}, A. Paramonov⁶, D. Paredes Hernandez¹⁷⁹, A.J. Parker⁷⁵, M.A. Parker³⁰, K.A. Parker⁴⁵, F. Parodi^{53a,53b}, J.A. Parsons³⁸, U. Parzefall⁵¹, V.R. Pascuzzi¹⁶¹, J.M. Pasner¹³⁹, E. Pasqualucci^{134a}, S. Passaggio^{53a}, Fr. Pastore⁸⁰, S. Pataia⁸⁶, J.R. Pater⁸⁷, T. Pauly³², B. Pearson¹⁰³, S. Pedraza Lopez¹⁷⁰, R. Pedro^{128a,128b}, S.V. Peleganchuk^{111,c}, O. Penc¹²⁹, C. Peng^{35a}, H. Peng^{36a}, J. Penwell⁶⁴, B.S. Peralva^{26b}, M.M. Perego¹³⁸, D.V. Perepelitsa²⁷, F. Peri¹⁷, L. Perini^{94a,94b}, H. Pernegger³², S. Perrella^{106a,106b}, R. Peschke⁴⁵, V.D. Peshekhonov^{68,*}, K. Peters⁴⁵, R.F.Y. Peters⁸⁷, B.A. Petersen³², T.C. Petersen³⁹, E. Petit⁵⁸, A. Petridis¹, C. Petridou¹⁵⁶, P. Petroff¹¹⁹, E. Petrolo^{134a}, M. Petrov¹²², F. Petrucci^{136a,136b}, N.E. Pettersson⁸⁹, A. Peyaud¹³⁸, R. Pezoa^{34b}, F.H. Phillips⁹³, P.W. Phillips¹³³, G. Piacquadio¹⁵⁰, E. Pianori¹⁷³, A. Picazio⁸⁹, M.A. Pickering¹²², R. Piegaia²⁹, J.E. Pilcher³³, A.D. Pilkington⁸⁷, M. Pinamonti^{135a,135b}, J.L. Pinfold³, H. Pirumov⁴⁵, M. Pitt¹⁷⁵, L. Plazak^{146a}, M.-A. Pleier²⁷, V. Pleskot⁸⁶, E. Plotnikova⁶⁸, D. Pluth⁶⁷, P. Podberezko¹¹¹, R. Poettgen⁸⁴, R. Poggi^{123a,123b}, L. Poggioli¹¹⁹, I. Pogrebnyak⁹³, D. Pohl²³, I. Pokharel⁵⁷, G. Polesello^{123a}, A. Poley⁴⁵, A. Policicchio^{40a,40b}, R. Polifka³², A. Polini^{22a}, C.S. Pollard⁵⁶, V. Polychronakos²⁷, K. Pommès³², D. Ponomarenko¹⁰⁰, L. Pontecorvo^{134a}, G.A. Popeneciu^{28d}, D.M. Portillo Quintero⁸³, S. Pospisil¹³⁰, K. Potamianos⁴⁵, I.N. Potrap⁶⁸, C.J. Potter³⁰, H. Potti¹¹, T. Poulsen⁸⁴, J. Poveda³², M.E. Pozo Astigarraga³², P. Pralavorio⁸⁸, A. Pranko¹⁶, S. Prell⁶⁷, D. Price⁸⁷, M. Primavera^{76a}, S. Prince⁹⁰, N. Proklova¹⁰⁰, K. Prokofiev^{62c}, F. Prokoshin^{34b}, S. Protopopescu²⁷, J. Proudfoot⁶, M. Przybycien^{41a}, A. Puri¹⁶⁹, P. Puzo¹¹⁹, J. Qian⁹², G. Qin⁵⁶, Y. Qin⁸⁷, A. Quadt⁵⁷, M. Queitsch-Maitland⁴⁵, D. Quilty⁵⁶, S. Raddum¹²¹, V. Radeka²⁷, V. Radescu¹²², S.K. Radhakrishnan¹⁵⁰, P. Radloff¹¹⁸, P. Rados⁹¹, F. Ragusa^{94a,94b}, G. Rahal¹⁸¹, J.A. Raine⁸⁷, S. Rajagopalan²⁷, C. Rangel-Smith¹⁶⁸, T. Rashid¹¹⁹, S. Raspopov⁵, M.G. Ratti^{94a,94b}, D.M. Rauch⁴⁵, F. Rauscher¹⁰², S. Rave⁸⁶, I. Ravinovich¹⁷⁵, J.H. Rawling⁸⁷, M. Raymond³², A.L. Read¹²¹, N.P. Readoff⁵⁸, M. Reale^{76a,76b}, D.M. Rebuzzi^{123a,123b}, A. Redelbach¹⁷⁷, G. Redlinger²⁷, R. Reece¹³⁹, R.G. Reed^{147c}, K. Reeves⁴⁴, L. Rehnisch¹⁷, J. Reichert¹²⁴, A. Reiss⁸⁶, C. Rembser³², H. Ren^{35a}, M. Rescigno^{134a}, S. Resconi^{94a}, E.D. Resseguie¹²⁴, S. Rettie¹⁷¹, E. Reynolds¹⁹, O.L. Rezanova^{111,c}, P. Reznicek¹³¹, R. Rezvani⁹⁷, R. Richter¹⁰³, S. Richter⁸¹, E. Richter-Was^{41b}, O. Ricken²³, M. Ridel⁸³, P. Rieck¹⁰³, C.J. Riegel¹⁷⁸, J. Rieger⁵⁷, O. Rifki¹¹⁵, M. Rijssenbeek¹⁵⁰, A. Rimoldi^{123a,123b}, M. Rimoldi¹⁸, L. Rinaldi^{22a},

G. Ripellino¹⁴⁹, B. Ristić³², E. Ritsch³², I. Riu¹³, F. Rizatdinova¹¹⁶, E. Rizvi⁷⁹, C. Rizzi¹³, R.T. Roberts⁸⁷, S.H. Robertson^{90,o}, A. Robichaud-Veronneau⁹⁰, D. Robinson³⁰, J.E.M. Robinson⁴⁵, A. Robson⁵⁶, E. Rocco⁸⁶, C. Roda^{126a,126b}, Y. Rodina^{88,al}, S. Rodriguez Bosca¹⁷⁰, A. Rodriguez Perez¹³, D. Rodriguez Rodriguez¹⁷⁰, S. Roe³², C.S. Rogan⁵⁹, O. Røhne¹²¹, J. Roloff⁵⁹, A. Romaniouk¹⁰⁰, M. Romano^{22a,22b}, S.M. Romano Saez³⁷, E. Romero Adam¹⁷⁰, N. Rompotis⁷⁷, M. Ronzani⁵¹, L. Roos⁸³, S. Rosati^{134a}, K. Rosbach⁵¹, P. Rose¹³⁹, N.-A. Rosien⁵⁷, E. Rossi^{106a,106b}, L.P. Rossi^{53a}, J.H.N. Rosten³⁰, R. Rosten¹⁴⁰, M. Rotaru^{28b}, J. Rothberg¹⁴⁰, D. Rousseau¹¹⁹, A. Rozanov⁸⁸, Y. Rozen¹⁵⁴, X. Ruan^{147c}, F. Rubbo¹⁴⁵, E.M. Ruettinger⁴⁵, F. Rühr⁵¹, A. Ruiz-Martinez³¹, Z. Rurikova⁵¹, N.A. Rusakovich⁶⁸, H.L. Russell⁹⁰, J.P. Rutherford⁷, N. Ruthmann³², Y.F. Ryabov¹²⁵, M. Rybar¹⁶⁹, G. Rybkin¹¹⁹, S. Ryu⁶, A. Ryzhov¹³², G.F. Rzehorz⁵⁷, A.F. Saavedra¹⁵², G. Sabato¹⁰⁹, S. Sacerdoti²⁹, H.F-W. Sadrozinski¹³⁹, R. Sadykov⁶⁸, F. Safai Tehrani^{134a}, P. Saha¹¹⁰, M. Sahinsoy^{60a}, M. Saimpert⁴⁵, M. Saito¹⁵⁷, T. Saito¹⁵⁷, H. Sakamoto¹⁵⁷, Y. Sakurai¹⁷⁴, G. Salamanna^{136a,136b}, J.E. Salazar Loyola^{34b}, D. Salek¹⁰⁹, P.H. Sales De Bruin¹⁶⁸, D. Salihagic¹⁰³, A. Salnikov¹⁴⁵, J. Salt¹⁷⁰, D. Salvatore^{40a,40b}, F. Salvatore¹⁵¹, A. Salvucci^{62a,62b,62c}, A. Salzburger³², D. Sammel⁵¹, D. Sampsonidis¹⁵⁶, D. Sampsonidou¹⁵⁶, J. Sánchez¹⁷⁰, V. Sanchez Martinez¹⁷⁰, A. Sanchez Pineda^{167a,167c}, H. Sandaker¹²¹, R.L. Sandbach⁷⁹, C.O. Sander⁴⁵, M. Sandhoff¹⁷⁸, C. Sandoval²¹, D.P.C. Sankey¹³³, M. Sannino^{53a,53b}, Y. Sano¹⁰⁵, A. Sansoni⁵⁰, C. Santoni³⁷, H. Santos^{128a}, I. Santoyo Castillo¹⁵¹, A. Saponov⁶⁸, J.G. Saraiva^{128a,128d}, B. Sarrazin²³, O. Sasaki⁶⁹, K. Sato¹⁶⁴, E. Sauvan⁵, G. Savage⁸⁰, P. Savard^{161,d}, N. Savic¹⁰³, C. Sawyer¹³³, L. Sawyer^{82,u}, J. Saxon³³, C. Sbarra^{22a}, A. Sbrizzi^{22a,22b}, T. Scanlon⁸¹, D.A. Scannicchio¹⁶⁶, J. Schaarschmidt¹⁴⁰, P. Schacht¹⁰³, B.M. Schachtner¹⁰², D. Schaefer³³, L. Schaefer¹²⁴, R. Schaefer⁴⁵, J. Schaeffer⁸⁶, S. Schaepe³², S. Schaezel^{60b}, U. Schäfer⁸⁶, A.C. Schaffer¹¹⁹, D. Schaile¹⁰², R.D. Schamberger¹⁵⁰, V.A. Schegelsky¹²⁵, D. Scheirich¹³¹, M. Schernau¹⁶⁶, C. Schiavi^{53a,53b}, S. Schier¹³⁹, L.K. Schildgen²³, C. Schillo⁵¹, M. Schioppa^{40a,40b}, S. Schlenker³², K.R. Schmidt-Sommerfeld¹⁰³, K. Schmieden³², C. Schmitt⁸⁶, S. Schmitt⁴⁵, S. Schmitz⁸⁶, U. Schnoor⁵¹, L. Schoeffel¹³⁸, A. Schoening^{60b}, B.D. Schoenrock⁹³, E. Schopf²³, M. Schott⁸⁶, J.F.P. Schouwenberg¹⁰⁸, J. Schovancova³², S. Schramm⁵², N. Schuh⁸⁶, A. Schulte⁸⁶, M.J. Schultens²³, H.-C. Schultz-Coulon^{60a}, H. Schulz¹⁷, M. Schumacher⁵¹, B.A. Schumm¹³⁹, Ph. Schune¹³⁸, A. Schwartzman¹⁴⁵, T.A. Schwarz⁹², H. Schweiger⁸⁷, Ph. Schwemling¹³⁸, R. Schwienhorst⁹³, J. Schwindling¹³⁸, A. Sciandra²³, G. Sciolla²⁵, M. Scornajenghi^{40a,40b}, F. Scuri^{126a,126b}, F. Scutti⁹¹, J. Searcy⁹², P. Seema²³, S.C. Seidel¹⁰⁷, A. Seiden¹³⁹, J.M. Seixas^{26a}, G. Sekhniaidze^{106a}, K. Sekhon⁹², S.J. Sekula⁴³, N. Semprini-Cesari^{22a,22b}, S. Senkin³⁷, C. Serfon¹²¹, L. Serin¹¹⁹, L. Serkin^{167a,167b}, M. Sessa^{136a,136b}, R. Seuster¹⁷², H. Severini¹¹⁵, T. Sfiligoj⁷⁸, F. Sforza¹⁶⁵, A. Sfyrla⁵², E. Shabalina⁵⁷, N.W. Shaikh^{148a,148b}, L.Y. Shan^{35a}, R. Shang¹⁶⁹, J.T. Shank²⁴, M. Shapiro¹⁶, P.B. Shatalov⁹⁹, K. Shaw^{167a,167b}, S.M. Shaw⁸⁷, A. Shcherbakova^{148a,148b}, C.Y. Shehu¹⁵¹, Y. Shen¹¹⁵, N. Sherafati³¹, P. Sherwood⁸¹, L. Shi^{153,am}, S. Shimizu⁷⁰, C.O. Shimmmin¹⁷⁹, M. Shimojima¹⁰⁴, I.P.J. Shipsey¹²², S. Shirabe⁷³, M. Shiyakova^{68,an}, J. Shlomi¹⁷⁵, A. Shmeleva⁹⁸, D. Shoaleh Saadi⁹⁷, M.J. Shochet³³, S. Shojaii^{94a,94b}, D.R. Shope¹¹⁵, S. Shrestha¹¹³, E. Shulga¹⁰⁰, M.A. Shupe⁷, P. Sicho¹²⁹, A.M. Sickles¹⁶⁹, P.E. Sidebo¹⁴⁹, E. Sideras Haddad^{147c}, O. Sidiropoulou¹⁷⁷, A. Sidoti^{22a,22b}, F. Siegert⁴⁷, Dj. Sijacki¹⁴, J. Silva^{128a,128d}, S.B. Silverstein^{148a}, V. Simak¹³⁰, Lj. Simic⁶⁸, S. Simion¹¹⁹, E. Simioni⁸⁶, B. Simmons⁸¹, M. Simon⁸⁶, P. Sinervo¹⁶¹, N.B. Sinev¹¹⁸, M. Sioli^{22a,22b}, G. Siragusa¹⁷⁷, I. Siral⁹², S.Yu. Sivoklov¹⁰¹, J. Sjölín^{148a,148b}, M.B. Skinner⁷⁵, P. Skubic¹¹⁵, M. Slater¹⁹, T. Slavicek¹³⁰, M. Slawinska⁴², K. Sliwa¹⁶⁵, R. Slovak¹³¹, V. Smakhtin¹⁷⁵, B.H. Smart⁵, J. Smiesko^{146a}, N. Smirnov¹⁰⁰, S.Yu. Smirnov¹⁰⁰, Y. Smirnov¹⁰⁰, L.N. Smirnova^{101,ao}, O. Smirnova⁸⁴, J.W. Smith⁵⁷, M.N.K. Smith³⁸, R.W. Smith³⁸, M. Smizanska⁷⁵, K. Smolek¹³⁰, A.A. Snesarev⁹⁸, I.M. Snyder¹¹⁸, S. Snyder²⁷, R. Sobie^{172,o}, F. Socher⁴⁷, A. Soffer¹⁵⁵, A. Søgaard⁴⁹, D.A. Soh¹⁵³, G. Sokhrannyi⁷⁸, C.A. Solans Sanchez³², M. Solar¹³⁰, E.Yu. Soldatov¹⁰⁰, U. Soldevila¹⁷⁰, A.A. Solodkov¹³², A. Soloshenko⁶⁸, O.V. Solovyanov¹³², V. Solovyev¹²⁵, P. Sommer¹⁴¹, H. Son¹⁶⁵, A. Sopczak¹³⁰, D. Sosa^{60b}, C.L. Sotiropoulou^{126a,126b}, S. Sottocornola^{123a,123b}, R. Soualah^{167a,167c}, A.M. Soukharev^{111,c}, D. South⁴⁵, B.C. Sowden⁸⁰, S. Spagnolo^{76a,76b}, M. Spalla^{126a,126b}, M. Spangenberg¹⁷³, F. Spanò⁸⁰, D. Sperlich¹⁷, F. Spettel¹⁰³, T.M. Spieker^{60a}, R. Spighi^{22a}, G. Spigo³², L.A. Spiller⁹¹, M. Spousta¹³¹, R.D. St. Denis^{56,*}, A. Stabile^{94a}, R. Stamen^{60a}, S. Stamm¹⁷, E. Stanecka⁴², R.W. Stanek⁶, C. Stancu^{136a}, M.M. Stanitzki⁴⁵, B.S. Stapf¹⁰⁹, S. Stapnes¹²¹, E.A. Starchenko¹³², G.H. Stark³³, J. Stark⁵⁸, S.H. Stark³⁹, P. Staroba¹²⁹, P. Starovoitov^{60a}, S. Stärz³², R. Staszewski⁴², M. Stegler⁴⁵, P. Steinberg²⁷, B. Stelzer¹⁴⁴,

H.J. Stelzer³², O. Stelzer-Chilton^{163a}, H. Stenzel⁵⁵, T.J. Stevenson⁷⁹, G.A. Stewart⁵⁶, M.C. Stockton¹¹⁸, M. Stoebe⁹⁰, G. Stoicea^{28b}, P. Stolte⁵⁷, S. Stonjek¹⁰³, A.R. Stradling⁸, A. Straessner⁴⁷, M.E. Stramaglia¹⁸, J. Strandberg¹⁴⁹, S. Strandberg^{148a,148b}, M. Strauss¹¹⁵, P. Strizenec^{146b}, R. Ströhmer¹⁷⁷, D.M. Strom¹¹⁸, R. Stroynowski⁴³, A. Strubig⁴⁹, S.A. Stucci²⁷, B. Stugu¹⁵, N.A. Styles⁴⁵, D. Su¹⁴⁵, J. Su¹²⁷, S. Suchek^{60a}, Y. Sugaya¹²⁰, M. Suk¹³⁰, V.V. Sulin⁹⁸, DMS Sultan^{162a,162b}, S. Sultansoy^{4c}, T. Sumida⁷¹, S. Sun⁵⁹, X. Sun³, K. Suruliz¹⁵¹, C.J.E. Suster¹⁵², M.R. Sutton¹⁵¹, S. Suzuki⁶⁹, M. Svatos¹²⁹, M. Swiatlowski³³, S.P. Swift², I. Sykora^{146a}, T. Sykora¹³¹, D. Ta⁵¹, K. Tackmann⁴⁵, J. Taenzer¹⁵⁵, A. Taffard¹⁶⁶, R. Tafiout^{163a}, E. Tahirovic⁷⁹, N. Taiblum¹⁵⁵, H. Takai²⁷, R. Takashima⁷², E.H. Takasugi¹⁰³, K. Takeda⁷⁰, T. Takeshita¹⁴², Y. Takubo⁶⁹, M. Talby⁸⁸, A.A. Talyshv^{111,c}, J. Tanaka¹⁵⁷, M. Tanaka¹⁵⁹, R. Tanaka¹¹⁹, S. Tanaka⁶⁹, R. Tanioka⁷⁰, B.B. Tannenwald¹¹³, S. Tapia Araya^{34b}, S. Tapprogge⁸⁶, S. Tarem¹⁵⁴, G.F. Tartarelli^{94a}, P. Tas¹³¹, M. Tasevsky¹²⁹, T. Tashiro⁷¹, E. Tassi^{40a,40b}, A. Tavares Delgado^{128a,128b}, Y. Tayalati^{137e}, A.C. Taylor¹⁰⁷, A.J. Taylor⁴⁹, G.N. Taylor⁹¹, P.T.E. Taylor⁹¹, W. Taylor^{163b}, P. Teixeira-Dias⁸⁰, D. Temple¹⁴⁴, H. Ten Kate³², P.K. Teng¹⁵³, J.J. Teoh¹²⁰, F. Tepel¹⁷⁸, S. Terada⁶⁹, K. Terasaki¹⁵⁷, J. Terron⁸⁵, S. Terzo¹³, M. Testa⁵⁰, R.J. Teuscher^{161,o}, S.J. Thais¹⁷⁹, T. Theveneaux-Pelzer⁸⁸, F. Thiele³⁹, J.P. Thomas¹⁹, J. Thomas-Wilsker⁸⁰, P.D. Thompson¹⁹, A.S. Thompson⁵⁶, L.A. Thomsen¹⁷⁹, E. Thomson¹²⁴, Y. Tian³⁸, M.J. Tibbetts¹⁶, R.E. Ticse Torres⁵⁷, V.O. Tikhomirov^{98,ap}, Yu.A. Tikhonov^{111,c}, S. Timoshenko¹⁰⁰, P. Tipton¹⁷⁹, S. Tisserant⁸⁸, K. Todome¹⁵⁹, S. Todorova-Nova⁵, S. Todt⁴⁷, J. Tojo⁷³, S. Tokár^{146a}, K. Tokushuku⁶⁹, E. Tolley⁵⁹, L. Tomlinson⁸⁷, M. Tomoto¹⁰⁵, L. Tompkins^{145,aq}, K. Toms¹⁰⁷, B. Tong⁵⁹, P. Tornambe⁵¹, E. Torrence¹¹⁸, H. Torres⁴⁷, E. Torró Pastor¹⁴⁰, J. Toth^{88,ar}, F. Touchard⁸⁸, D.R. Tovey¹⁴¹, C.J. Treado¹¹², T. Trefzger¹⁷⁷, F. Tresoldi¹⁵¹, A. Tricoli²⁷, I.M. Trigger^{163a}, S. Trincas-Duvoid⁸³, M.F. Tripiana¹³, W. Trischuk¹⁶¹, B. Trocme⁵⁸, A. Trofymov⁴⁵, C. Troncon^{94a}, M. Trottier-McDonald¹⁶, M. Trovatelli¹⁷², L. Truong^{147b}, M. Trzebinski⁴², A. Trzupek⁴², K.W. Tsang^{62a}, J.C.-L. Tseng¹²², P.V. Tsiarehka⁹⁵, G. Tsipolitis¹⁰, N. Tsirintanis⁹, S. Tsiskaridze¹³, V. Tsiskaridze⁵¹, E.G. Tskhadadze^{54a}, I.I. Tsukerman⁹⁹, V. Tsulaia¹⁶, S. Tsuno⁶⁹, D. Tsybychev¹⁵⁰, Y. Tu^{62b}, A. Tudorache^{28b}, V. Tudorache^{28b}, T.T. Tulbure^{28a}, A.N. Tuna⁵⁹, S. Turchikhin⁶⁸, D. Turgeman¹⁷⁵, I. Turk Cakir^{4b,as}, R. Turra^{94a}, P.M. Tuts³⁸, G. Ucchielli^{22a,22b}, I. Ueda⁶⁹, M. Ughetto^{148a,148b}, F. Ukegawa¹⁶⁴, G. Unal³², A. Undrus²⁷, G. Unel¹⁶⁶, F.C. Ungaro⁹¹, Y. Unno⁶⁹, K. Uno¹⁵⁷, C. Unverdorben¹⁰², J. Urban^{146b}, P. Urquijo⁹¹, P. Urrejola⁸⁶, G. Usai⁸, J. Usui⁶⁹, L. Vacavant⁸⁸, V. Vacek¹³⁰, B. Vachon⁹⁰, K.O.H. Vadla¹²¹, A. Vaidya⁸¹, C. Valderanis¹⁰², E. Valdes Santurio^{148a,148b}, M. Valente⁵², S. Valentini^{22a,22b}, A. Valero¹⁷⁰, L. Valéry¹³, S. Valkar¹³¹, A. Vallier⁵, J.A. Valls Ferrer¹⁷⁰, W. Van Den Wollenberg¹⁰⁹, H. van der Graaf¹⁰⁹, P. van Gemmeren⁶, J. Van Nieuwkoop¹⁴⁴, I. van Vulpen¹⁰⁹, M.C. van Woerden¹⁰⁹, M. Vanadia^{135a,135b}, W. Vandelli³², A. Vaniachine¹⁶⁰, P. Vankov¹⁰⁹, G. Vardanyan¹⁸⁰, R. Vari^{134a}, E.W. Varnes⁷, C. Varni^{53a,53b}, T. Varol⁴³, D. Varouchas¹¹⁹, A. Vartapetian⁸, K.E. Varvell¹⁵², J.G. Vasquez¹⁷⁹, G.A. Vasquez^{34b}, F. Vazeille³⁷, D. Vazquez Furelos¹³, T. Vazquez Schroeder⁹⁰, J. Veatch⁵⁷, V. Veeraraghavan⁷, L.M. Veloce¹⁶¹, F. Veloso^{128a,128c}, S. Veneziano^{134a}, A. Ventura^{76a,76b}, M. Venturi¹⁷², N. Venturi³², A. Venturini²⁵, V. Vercesi^{123a}, M. Verducci^{136a,136b}, W. Verkerke¹⁰⁹, A.T. Vermeulen¹⁰⁹, J.C. Vermeulen¹⁰⁹, M.C. Vetterli^{144,d}, N. Viaux Maira^{34b}, O. Viazlo⁸⁴, I. Vichou^{169,*}, T. Vickey¹⁴¹, O.E. Vickey Boeriu¹⁴¹, G.H.A. Viehhauser¹²², S. Viel¹⁶, L. Viganì¹²², M. Villa^{22a,22b}, M. Villaplana Perez^{94a,94b}, E. Vilucchi⁵⁰, M.G. Vinciter³¹, V.B. Vinogradov⁶⁸, A. Vishwakarma⁴⁵, C. Vittori^{22a,22b}, I. Vivarelli¹⁵¹, S. Vlachos¹⁰, M. Vogel¹⁷⁸, P. Vokac¹³⁰, G. Volpi¹³, H. von der Schmitt¹⁰³, E. von Toerne²³, V. Vorobel¹³¹, K. Vorobev¹⁰⁰, M. Vos¹⁷⁰, R. Voss³², J.H. Vosseveld⁷⁷, N. Vranjes¹⁴, M. Vranjes Milosavljevic¹⁴, V. Vrba¹³⁰, M. Vreeswijk¹⁰⁹, R. Vuillermet³², I. Vukotic³³, P. Wagner²³, W. Wagner¹⁷⁸, J. Wagner-Kuhr¹⁰², H. Wahlberg⁷⁴, S. Wahrmond⁴⁷, J. Walder⁷⁵, R. Walker¹⁰², W. Walkowiak¹⁴³, V. Wallangen^{148a,148b}, C. Wang^{35b}, C. Wang^{36b,at}, F. Wang¹⁷⁶, H. Wang¹⁶, H. Wang³, J. Wang⁴⁵, J. Wang¹⁵², Q. Wang¹¹⁵, R.-J. Wang⁸³, R. Wang⁶, S.M. Wang¹⁵³, T. Wang³⁸, W. Wang^{153,au}, W. Wang^{36a,av}, Z. Wang^{36c}, C. Wanotayaroj⁴⁵, A. Warburton⁹⁰, C.P. Ward³⁰, D.R. Wardrope⁸¹, A. Washbrook⁴⁹, P.M. Watkins¹⁹, A.T. Watson¹⁹, M.F. Watson¹⁹, G. Watts¹⁴⁰, S. Watts⁸⁷, B.M. Waugh⁸¹, A.F. Webb¹¹, S. Webb⁸⁶, M.S. Weber¹⁸, S.M. Weber^{60a}, S.W. Weber¹⁷⁷, S.A. Weber³¹, J.S. Webster⁶, A.R. Weidberg¹²², B. Weinert⁶⁴, J. Weingarten⁵⁷, M. Weirich⁸⁶, C. Weiser⁵¹, H. Weits¹⁰⁹, P.S. Wells³², T. Wenaus²⁷, T. Wengler³², S. Wenig³², N. Vermes²³, M.D. Werner⁶⁷, P. Werner³², M. Wessels^{60a}, T.D. Weston¹⁸, K. Whalen¹¹⁸, N.L. Whallon¹⁴⁰, A.M. Wharton⁷⁵, A.S. White⁹², A. White⁸, M.J. White¹,

R. White^{34b}, D. Whiteson¹⁶⁶, B.W. Whitmore⁷⁵, F.J. Wickens¹³³, W. Wiedenmann¹⁷⁶, M. Wielers¹³³, C. Wiglesworth³⁹, L.A.M. Wiik-Fuchs⁵¹, A. Wildauer¹⁰³, F. Wilk⁸⁷, H.G. Wilkens³², H.H. Williams¹²⁴, S. Williams¹⁰⁹, C. Willis⁹³, S. Willocq⁸⁹, J.A. Wilson¹⁹, I. Wingerter-Seez⁵, E. Winkels¹⁵¹, F. Winklmeier¹¹⁸, O.J. Winston¹⁵¹, B.T. Winter²³, M. Wittgen¹⁴⁵, M. Wobisch^{82,u}, T.M.H. Wolf¹⁰⁹, R. Wolff⁸⁸, M.W. Wolter⁴², H. Wolters^{128a,128c}, V.W.S. Wong¹⁷¹, N.L. Woods¹³⁹, S.D. Worm¹⁹, B.K. Wosiek⁴², J. Wotschack³², K.W. Wozniak⁴², M. Wu³³, S.L. Wu¹⁷⁶, X. Wu⁵², Y. Wu⁹², T.R. Wyatt⁸⁷, B.M. Wynne⁴⁹, S. Xella³⁹, Z. Xi⁹², L. Xia^{35c}, D. Xu^{35a}, L. Xu²⁷, T. Xu¹³⁸, W. Xu⁹², B. Yabsley¹⁵², S. Yacoub^{147a}, D. Yamaguchi¹⁵⁹, Y. Yamaguchi¹⁵⁹, A. Yamamoto⁶⁹, S. Yamamoto¹⁵⁷, T. Yamanaka¹⁵⁷, F. Yamane⁷⁰, M. Yamatani¹⁵⁷, T. Yamazaki¹⁵⁷, Y. Yamazaki⁷⁰, Z. Yan²⁴, H. Yang^{36c}, H. Yang¹⁶, Y. Yang¹⁵³, Z. Yang¹⁵, W.-M. Yao¹⁶, Y.C. Yap⁴⁵, Y. Yasu⁶⁹, E. Yatsenko⁵, K.H. Yau Wong²³, J. Ye⁴³, S. Ye²⁷, I. Yeletsikh⁶⁸, E. Yigitbasi²⁴, E. Yildirim⁸⁶, K. Yorita¹⁷⁴, K. Yoshihara¹²⁴, C. Young¹⁴⁵, C.J.S. Young³², J. Yu⁸, J. Yu⁶⁷, S.P.Y. Yuen²³, I. Yusuf^{30,aw}, B. Zabinski⁴², G. Zacharis¹⁰, R. Zaidan¹³, A.M. Zaitsev^{132,aj}, N. Zakharchuk⁴⁵, J. Zalieckas¹⁵, A. Zaman¹⁵⁰, S. Zambito⁵⁹, D. Zanzi⁹¹, C. Zeitnitz¹⁷⁸, G. Zemaityte¹²², A. Zemla^{41a}, J.C. Zeng¹⁶⁹, Q. Zeng¹⁴⁵, O. Zenin¹³², T. Ženiš^{146a}, D. Zerwas¹¹⁹, D. Zhang^{36b}, D. Zhang⁹², F. Zhang¹⁷⁶, G. Zhang^{36a,av}, H. Zhang¹¹⁹, J. Zhang⁶, L. Zhang⁵¹, L. Zhang^{36a}, M. Zhang¹⁶⁹, P. Zhang^{35b}, R. Zhang²³, R. Zhang^{36a,at}, X. Zhang^{36b}, Y. Zhang^{35a}, Z. Zhang¹¹⁹, X. Zhao⁴³, Y. Zhao^{36b,ax}, Z. Zhao^{36a}, A. Zhemchugov⁶⁸, B. Zhou⁹², C. Zhou¹⁷⁶, L. Zhou⁴³, M. Zhou^{35a}, M. Zhou¹⁵⁰, N. Zhou^{36c}, C.G. Zhu^{36b}, H. Zhu^{35a}, J. Zhu⁹², Y. Zhu^{36a}, X. Zhuang^{35a}, K. Zhukov⁹⁸, A. Zibell¹⁷⁷, D. Zieminska⁶⁴, N.I. Zimine⁶⁸, C. Zimmermann⁸⁶, S. Zimmermann⁵¹, Z. Zinonos¹⁰³, M. Zinser⁸⁶, M. Ziolkowski¹⁴³, L. Živković¹⁴, G. Zobernig¹⁷⁶, A. Zoccoli^{22a,22b}, R. Zou³³, M. zur Nedden¹⁷, L. Zwalinski³²

¹ Department of Physics, University of Adelaide, Adelaide, Australia

² Physics Department, SUNY Albany, Albany NY, United States

³ Department of Physics, University of Alberta, Edmonton AB, Canada

⁴ (a) Department of Physics, Ankara University, Ankara; (b) Istanbul Aydin University, Istanbul; (c) Division of Physics, TOBB University of Economics and Technology, Ankara, Turkey

⁵ LAPP, CNRS/IN2P3 and Université Savoie Mont Blanc, Annecy-le-Vieux, France

⁶ High Energy Physics Division, Argonne National Laboratory, Argonne IL, United States

⁷ Department of Physics, University of Arizona, Tucson AZ, United States

⁸ Department of Physics, The University of Texas at Arlington, Arlington TX, United States

⁹ Physics Department, National and Kapodistrian University of Athens, Athens, Greece

¹⁰ Physics Department, National Technical University of Athens, Zografou, Greece

¹¹ Department of Physics, The University of Texas at Austin, Austin TX, United States

¹² Institute of Physics, Azerbaijan Academy of Sciences, Baku, Azerbaijan

¹³ Institut de Física d'Altes Energies (IFAE), The Barcelona Institute of Science and Technology, Barcelona, Spain

¹⁴ Institute of Physics, University of Belgrade, Belgrade, Serbia

¹⁵ Department for Physics and Technology, University of Bergen, Bergen, Norway

¹⁶ Physics Division, Lawrence Berkeley National Laboratory and University of California, Berkeley CA, United States

¹⁷ Department of Physics, Humboldt University, Berlin, Germany

¹⁸ Albert Einstein Center for Fundamental Physics and Laboratory for High Energy Physics, University of Bern, Bern, Switzerland

¹⁹ School of Physics and Astronomy, University of Birmingham, Birmingham, United Kingdom

²⁰ (a) Department of Physics, Bogazici University, Istanbul; (b) Department of Physics Engineering, Gaziantep University, Gaziantep; (d) Istanbul Bilgi University, Faculty of Engineering and Natural Sciences, Istanbul; (e) Bahcesehir University, Faculty of Engineering and Natural Sciences, Istanbul, Turkey

²¹ Centro de Investigaciones, Universidad Antonio Narino, Bogota, Colombia

²² (a) INFN Sezione di Bologna; (b) Dipartimento di Fisica e Astronomia, Università di Bologna, Bologna, Italy

²³ Physikalisches Institut, University of Bonn, Bonn, Germany

²⁴ Department of Physics, Boston University, Boston MA, United States

²⁵ Department of Physics, Brandeis University, Waltham MA, United States

²⁶ (a) Universidade Federal do Rio De Janeiro COPPE/EE/IF, Rio de Janeiro; (b) Electrical Circuits Department, Federal University of Juiz de Fora (UFJF), Juiz de Fora; (c) Federal University of Sao Joao del Rei (UFSJ), Sao Joao del Rei; (d) Instituto de Fisica, Universidade de Sao Paulo, Sao Paulo, Brazil

²⁷ Physics Department, Brookhaven National Laboratory, Upton NY, United States

²⁸ (a) Transilvania University of Brasov, Brasov; (b) Horia Hulubei National Institute of Physics and Nuclear Engineering, Bucharest; (c) Department of Physics, Alexandru Ioan Cuza University of Iasi, Iasi; (d) National Institute for Research and Development of Isotopic and Molecular Technologies, Physics Department, Cluj Napoca; (e) University Politehnica Bucharest, Bucharest; (f) West University in Timisoara, Timisoara, Romania

²⁹ Departamento de Fisica, Universidad de Buenos Aires, Buenos Aires, Argentina

³⁰ Cavendish Laboratory, University of Cambridge, Cambridge, United Kingdom

³¹ Department of Physics, Carleton University, Ottawa ON, Canada

³² CERN, Geneva, Switzerland

³³ Enrico Fermi Institute, University of Chicago, Chicago IL, United States

³⁴ (a) Departamento de Fisica, Pontificia Universidad Católica de Chile, Santiago; (b) Departamento de Fisica, Universidad Técnica Federico Santa María, Valparaíso, Chile

³⁵ (a) Institute of High Energy Physics, Chinese Academy of Sciences, Beijing; (b) Department of Physics, Nanjing University, Jiangsu; (c) Physics Department, Tsinghua University, Beijing 100084, China

³⁶ (a) Department of Modern Physics and State Key Laboratory of Particle Detection and Electronics, University of Science and Technology of China, Anhui; (b) School of Physics, Shandong University, Shandong; (c) Department of Physics and Astronomy, Key Laboratory for Particle Physics, Astrophysics and Cosmology, Ministry of Education; Shanghai Key Laboratory for Particle Physics and Cosmology, Shanghai Jiao Tong University, Shanghai (also at PKU-CHEP), China

³⁷ Université Clermont Auvergne, CNRS/IN2P3, LPC, Clermont-Ferrand, France

³⁸ Nevis Laboratory, Columbia University, Irvington NY, United States

³⁹ Niels Bohr Institute, University of Copenhagen, Copenhagen, Denmark

- ⁴⁰ (a) INFN Gruppo Collegato di Cosenza, Laboratori Nazionali di Frascati; (b) Dipartimento di Fisica, Università della Calabria, Rende, Italy
- ⁴¹ (a) AGH University of Science and Technology, Faculty of Physics and Applied Computer Science, Krakow; (b) Marian Smoluchowski Institute of Physics, Jagiellonian University, Krakow, Poland
- ⁴² Institute of Nuclear Physics Polish Academy of Sciences, Krakow, Poland
- ⁴³ Physics Department, Southern Methodist University, Dallas TX, United States
- ⁴⁴ Physics Department, University of Texas at Dallas, Richardson TX, United States
- ⁴⁵ DESY, Hamburg and Zeuthen, Germany
- ⁴⁶ Lehrstuhl für Experimentelle Physik IV, Technische Universität Dortmund, Dortmund, Germany
- ⁴⁷ Institut für Kern- und Teilchenphysik, Technische Universität Dresden, Dresden, Germany
- ⁴⁸ Department of Physics, Duke University, Durham NC, United States
- ⁴⁹ SUPA – School of Physics and Astronomy, University of Edinburgh, Edinburgh, United Kingdom
- ⁵⁰ INFN e Laboratori Nazionali di Frascati, Frascati, Italy
- ⁵¹ Fakultät für Mathematik und Physik, Albert-Ludwigs-Universität, Freiburg, Germany
- ⁵² Département de Physique Nucleaire et Corpusculaire, Université de Genève, Geneva, Switzerland
- ⁵³ (a) INFN Sezione di Genova; (b) Dipartimento di Fisica, Università di Genova, Genova, Italy
- ⁵⁴ (a) E. Andronikashvili Institute of Physics, Iv. Javakhishvili Tbilisi State University, Tbilisi; (b) High Energy Physics Institute, Tbilisi State University, Tbilisi, Georgia
- ⁵⁵ II Physikalisches Institut, Justus-Liebig-Universität Giessen, Giessen, Germany
- ⁵⁶ SUPA – School of Physics and Astronomy, University of Glasgow, Glasgow, United Kingdom
- ⁵⁷ II Physikalisches Institut, Georg-August-Universität, Göttingen, Germany
- ⁵⁸ Laboratoire de Physique Subatomique et de Cosmologie, Université Grenoble-Alpes, CNRS/IN2P3, Grenoble, France
- ⁵⁹ Laboratory for Particle Physics and Cosmology, Harvard University, Cambridge MA, United States
- ⁶⁰ (a) Kirchhoff-Institut für Physik, Ruprecht-Karls-Universität Heidelberg, Heidelberg; (b) Physikalisches Institut, Ruprecht-Karls-Universität Heidelberg, Heidelberg, Germany
- ⁶¹ Faculty of Applied Information Science, Hiroshima Institute of Technology, Hiroshima, Japan
- ⁶² (a) Department of Physics, The Chinese University of Hong Kong, Shatin, N.T., Hong Kong; (b) Department of Physics, The University of Hong Kong, Hong Kong; (c) Department of Physics and Institute for Advanced Study, The Hong Kong University of Science and Technology, Clear Water Bay, Kowloon, Hong Kong, China
- ⁶³ Department of Physics, National Tsing Hua University, Taiwan, Taiwan
- ⁶⁴ Department of Physics, Indiana University, Bloomington IN, United States
- ⁶⁵ Institut für Astro- und Teilchenphysik, Leopold-Franzens-Universität, Innsbruck, Austria
- ⁶⁶ University of Iowa, Iowa City IA, United States
- ⁶⁷ Department of Physics and Astronomy, Iowa State University, Ames IA, United States
- ⁶⁸ Joint Institute for Nuclear Research, JINR Dubna, Dubna, Russia
- ⁶⁹ KEK, High Energy Accelerator Research Organization, Tsukuba, Japan
- ⁷⁰ Graduate School of Science, Kobe University, Kobe, Japan
- ⁷¹ Faculty of Science, Kyoto University, Kyoto, Japan
- ⁷² Kyoto University of Education, Kyoto, Japan
- ⁷³ Research Center for Advanced Particle Physics and Department of Physics, Kyushu University, Fukuoka, Japan
- ⁷⁴ Instituto de Física La Plata, Universidad Nacional de La Plata and CONICET, La Plata, Argentina
- ⁷⁵ Physics Department, Lancaster University, Lancaster, United Kingdom
- ⁷⁶ (a) INFN Sezione di Lecce; (b) Dipartimento di Matematica e Fisica, Università del Salento, Lecce, Italy
- ⁷⁷ Oliver Lodge Laboratory, University of Liverpool, Liverpool, United Kingdom
- ⁷⁸ Department of Experimental Particle Physics, Jožef Stefan Institute and Department of Physics, University of Ljubljana, Ljubljana, Slovenia
- ⁷⁹ School of Physics and Astronomy, Queen Mary University of London, London, United Kingdom
- ⁸⁰ Department of Physics, Royal Holloway University of London, Surrey, United Kingdom
- ⁸¹ Department of Physics and Astronomy, University College London, London, United Kingdom
- ⁸² Louisiana Tech University, Ruston LA, United States
- ⁸³ Laboratoire de Physique Nucléaire et de Hautes Energies, UPMC and Université Paris-Diderot and CNRS/IN2P3, Paris, France
- ⁸⁴ Fysiska institutionen, Lunds universitet, Lund, Sweden
- ⁸⁵ Departamento de Física Teórica C-15, Universidad Autónoma de Madrid, Madrid, Spain
- ⁸⁶ Institut für Physik, Universität Mainz, Mainz, Germany
- ⁸⁷ School of Physics and Astronomy, University of Manchester, Manchester, United Kingdom
- ⁸⁸ CPPM, Aix-Marseille Université and CNRS/IN2P3, Marseille, France
- ⁸⁹ Department of Physics, University of Massachusetts, Amherst MA, United States
- ⁹⁰ Department of Physics, McGill University, Montreal QC, Canada
- ⁹¹ School of Physics, University of Melbourne, Victoria, Australia
- ⁹² Department of Physics, The University of Michigan, Ann Arbor MI, United States
- ⁹³ Department of Physics and Astronomy, Michigan State University, East Lansing MI, United States
- ⁹⁴ (a) INFN Sezione di Milano; (b) Dipartimento di Fisica, Università di Milano, Milano, Italy
- ⁹⁵ B.I. Stepanov Institute of Physics, National Academy of Sciences of Belarus, Minsk, Belarus
- ⁹⁶ Research Institute for Nuclear Problems of Byelorussian State University, Minsk, Belarus
- ⁹⁷ Group of Particle Physics, University of Montreal, Montreal QC, Canada
- ⁹⁸ P.N. Lebedev Physical Institute of the Russian Academy of Sciences, Moscow, Russia
- ⁹⁹ Institute for Theoretical and Experimental Physics (ITEP), Moscow, Russia
- ¹⁰⁰ National Research Nuclear University MEPhI, Moscow, Russia
- ¹⁰¹ D.V. Skobeltsyn Institute of Nuclear Physics, M.V. Lomonosov Moscow State University, Moscow, Russia
- ¹⁰² Fakultät für Physik, Ludwig-Maximilians-Universität München, München, Germany
- ¹⁰³ Max-Planck-Institut für Physik (Werner-Heisenberg-Institut), München, Germany
- ¹⁰⁴ Nagasaki Institute of Applied Science, Nagasaki, Japan
- ¹⁰⁵ Graduate School of Science and Kobayashi-Maskawa Institute, Nagoya University, Nagoya, Japan
- ¹⁰⁶ (a) INFN Sezione di Napoli; (b) Dipartimento di Fisica, Università di Napoli, Napoli, Italy
- ¹⁰⁷ Department of Physics and Astronomy, University of New Mexico, Albuquerque NM, United States
- ¹⁰⁸ Institute for Mathematics, Astrophysics and Particle Physics, Radboud University Nijmegen/Nikhef, Nijmegen, Netherlands
- ¹⁰⁹ Nikhef National Institute for Subatomic Physics and University of Amsterdam, Amsterdam, Netherlands
- ¹¹⁰ Department of Physics, Northern Illinois University, DeKalb IL, United States
- ¹¹¹ Budker Institute of Nuclear Physics, SB RAS, Novosibirsk, Russia
- ¹¹² Department of Physics, New York University, New York NY, United States
- ¹¹³ Ohio State University, Columbus OH, United States
- ¹¹⁴ Faculty of Science, Okayama University, Okayama, Japan
- ¹¹⁵ Homer L. Dodge Department of Physics and Astronomy, University of Oklahoma, Norman OK, United States
- ¹¹⁶ Department of Physics, Oklahoma State University, Stillwater OK, United States

- ¹¹⁷ Palacký University, RCPTM, Olomouc, Czech Republic
- ¹¹⁸ Center for High Energy Physics, University of Oregon, Eugene OR, United States
- ¹¹⁹ LAL, Univ. Paris-Sud, CNRS/IN2P3, Université Paris-Saclay, Orsay, France
- ¹²⁰ Graduate School of Science, Osaka University, Osaka, Japan
- ¹²¹ Department of Physics, University of Oslo, Oslo, Norway
- ¹²² Department of Physics, Oxford University, Oxford, United Kingdom
- ¹²³ ^(a) INFN Sezione di Pavia; ^(b) Dipartimento di Fisica, Università di Pavia, Pavia, Italy
- ¹²⁴ Department of Physics, University of Pennsylvania, Philadelphia PA, United States
- ¹²⁵ National Research Centre “Kurchatov Institute”, B.P. Konstantinov Petersburg Nuclear Physics Institute, St. Petersburg, Russia
- ¹²⁶ ^(a) INFN Sezione di Pisa; ^(b) Dipartimento di Fisica E. Fermi, Università di Pisa, Pisa, Italy
- ¹²⁷ Department of Physics and Astronomy, University of Pittsburgh, Pittsburgh PA, United States
- ¹²⁸ ^(a) Laboratório de Instrumentação e Física Experimental de Partículas – LIP, Lisboa; ^(b) Faculdade de Ciências, Universidade de Lisboa, Lisboa; ^(c) Department of Physics, University of Coimbra, Coimbra; ^(d) Centro de Física Nuclear da Universidade de Lisboa, Lisboa; ^(e) Departamento de Física, Universidade do Minho, Braga; ^(f) Departamento de Física Teórica y del Cosmos, Universidad de Granada, Granada; ^(g) Dep Física and CEFITEC of Faculdade de Ciências e Tecnologia, Universidade Nova de Lisboa, Caparica, Portugal
- ¹²⁹ Institute of Physics, Academy of Sciences of the Czech Republic, Praha, Czech Republic
- ¹³⁰ Czech Technical University in Prague, Praha, Czech Republic
- ¹³¹ Charles University, Faculty of Mathematics and Physics, Prague, Czech Republic
- ¹³² State Research Center Institute for High Energy Physics (Protvino), NRC KI, Russia
- ¹³³ Particle Physics Department, Rutherford Appleton Laboratory, Didcot, United Kingdom
- ¹³⁴ ^(a) INFN Sezione di Roma; ^(b) Dipartimento di Fisica, Sapienza Università di Roma, Roma, Italy
- ¹³⁵ ^(a) INFN Sezione di Roma Tor Vergata; ^(b) Dipartimento di Fisica, Università di Roma Tor Vergata, Roma, Italy
- ¹³⁶ ^(a) INFN Sezione di Roma Tre; ^(b) Dipartimento di Matematica e Fisica, Università Roma Tre, Roma, Italy
- ¹³⁷ ^(a) Faculté des Sciences Ain Chock, Réseau Universitaire de Physique des Hautes Energies – Université Hassan II, Casablanca; ^(b) Centre National de l’Energie des Sciences Techniques Nucleaires, Rabat; ^(c) Faculté des Sciences Semlalia, Université Cadi Ayyad, LPHEA-Marrakech; ^(d) Faculté des Sciences, Université Mohamed Premier and LPTPM, Oujda; ^(e) Faculté des sciences, Université Mohammed V, Rabat, Morocco
- ¹³⁸ DSM/IRFU (Institut de Recherches sur les Lois Fondamentales de l’Univers), CEA Saclay (Commissariat à l’Energie Atomique et aux Energies Alternatives), Gif-sur-Yvette, France
- ¹³⁹ Santa Cruz Institute for Particle Physics, University of California Santa Cruz, Santa Cruz CA, United States
- ¹⁴⁰ Department of Physics, University of Washington, Seattle WA, United States
- ¹⁴¹ Department of Physics and Astronomy, University of Sheffield, Sheffield, United Kingdom
- ¹⁴² Department of Physics, Shinshu University, Nagano, Japan
- ¹⁴³ Department Physik, Universität Siegen, Siegen, Germany
- ¹⁴⁴ Department of Physics, Simon Fraser University, Burnaby BC, Canada
- ¹⁴⁵ SLAC National Accelerator Laboratory, Stanford CA, United States
- ¹⁴⁶ ^(a) Faculty of Mathematics, Physics & Informatics, Comenius University, Bratislava; ^(b) Department of Subnuclear Physics, Institute of Experimental Physics of the Slovak Academy of Sciences, Kosice, Slovak Republic
- ¹⁴⁷ ^(a) Department of Physics, University of Cape Town, Cape Town; ^(b) Department of Physics, University of Johannesburg, Johannesburg; ^(c) School of Physics, University of the Witwatersrand, Johannesburg, South Africa
- ¹⁴⁸ ^(a) Department of Physics, Stockholm University; ^(b) The Oskar Klein Centre, Stockholm, Sweden
- ¹⁴⁹ Physics Department, Royal Institute of Technology, Stockholm, Sweden
- ¹⁵⁰ Departments of Physics & Astronomy and Chemistry, Stony Brook University, Stony Brook NY, United States
- ¹⁵¹ Department of Physics and Astronomy, University of Sussex, Brighton, United Kingdom
- ¹⁵² School of Physics, University of Sydney, Sydney, Australia
- ¹⁵³ Institute of Physics, Academia Sinica, Taipei, Taiwan
- ¹⁵⁴ Department of Physics, Technion: Israel Institute of Technology, Haifa, Israel
- ¹⁵⁵ Raymond and Beverly Sackler School of Physics and Astronomy, Tel Aviv University, Tel Aviv, Israel
- ¹⁵⁶ Department of Physics, Aristotle University of Thessaloniki, Thessaloniki, Greece
- ¹⁵⁷ International Center for Elementary Particle Physics and Department of Physics, The University of Tokyo, Tokyo, Japan
- ¹⁵⁸ Graduate School of Science and Technology, Tokyo Metropolitan University, Tokyo, Japan
- ¹⁵⁹ Department of Physics, Tokyo Institute of Technology, Tokyo, Japan
- ¹⁶⁰ Tomsk State University, Tomsk, Russia
- ¹⁶¹ Department of Physics, University of Toronto, Toronto ON, Canada
- ¹⁶² ^(a) INFN-TIFPA; ^(b) University of Trento, Trento, Italy
- ¹⁶³ ^(a) TRIUMF, Vancouver BC; ^(b) Department of Physics and Astronomy, York University, Toronto ON, Canada
- ¹⁶⁴ Faculty of Pure and Applied Sciences, and Center for Integrated Research in Fundamental Science and Engineering, University of Tsukuba, Tsukuba, Japan
- ¹⁶⁵ Department of Physics and Astronomy, Tufts University, Medford MA, United States
- ¹⁶⁶ Department of Physics and Astronomy, University of California Irvine, Irvine CA, United States
- ¹⁶⁷ ^(a) INFN Gruppo Collegato di Udine, Sezione di Trieste, Udine; ^(b) ICTP, Trieste; ^(c) Dipartimento di Chimica, Fisica e Ambiente, Università di Udine, Udine, Italy
- ¹⁶⁸ Department of Physics and Astronomy, University of Uppsala, Uppsala, Sweden
- ¹⁶⁹ Department of Physics, University of Illinois, Urbana IL, United States
- ¹⁷⁰ Instituto de Física Corpuscular (IFIC), Centro Mixto Universidad de Valencia – CSIC, Spain
- ¹⁷¹ Department of Physics, University of British Columbia, Vancouver BC, Canada
- ¹⁷² Department of Physics and Astronomy, University of Victoria, Victoria BC, Canada
- ¹⁷³ Department of Physics, University of Warwick, Coventry, United Kingdom
- ¹⁷⁴ Waseda University, Tokyo, Japan
- ¹⁷⁵ Department of Particle Physics, The Weizmann Institute of Science, Rehovot, Israel
- ¹⁷⁶ Department of Physics, University of Wisconsin, Madison WI, United States
- ¹⁷⁷ Fakultät für Physik und Astronomie, Julius-Maximilians-Universität, Würzburg, Germany
- ¹⁷⁸ Fakultät für Mathematik und Naturwissenschaften, Fachgruppe Physik, Bergische Universität Wuppertal, Wuppertal, Germany
- ¹⁷⁹ Department of Physics, Yale University, New Haven CT, United States
- ¹⁸⁰ Yerevan Physics Institute, Yerevan, Armenia
- ¹⁸¹ Centre de Calcul de l’Institut National de Physique Nucléaire et de Physique des Particules (IN2P3), Villeurbanne, France
- ¹⁸² Academia Sinica Grid Computing, Institute of Physics, Academia Sinica, Taipei, Taiwan

^a Also at Department of Physics, King’s College London, London, United Kingdom.

^b Also at Institute of Physics, Azerbaijan Academy of Sciences, Baku, Azerbaijan.

^c Also at Novosibirsk State University, Novosibirsk, Russia.

^d Also at TRIUMF, Vancouver BC, Canada.

^e Also at Department of Physics & Astronomy, University of Louisville, Louisville, KY, United States.

- ^f Also at Physics Department, An-Najah National University, Nablus, Palestine.
- ^g Also at Department of Physics, California State University, Fresno CA, United States.
- ^h Also at Department of Physics, University of Fribourg, Fribourg, Switzerland.
- ⁱ Also at II Physikalisches Institut, Georg-August-Universität, Göttingen, Germany.
- ^j Also at Departament de Física de la Universitat Autònoma de Barcelona, Barcelona, Spain.
- ^k Also at Departamento de Física e Astronomia, Faculdade de Ciências, Universidade do Porto, Portugal.
- ^l Also at Tomsk State University, Tomsk, and Moscow Institute of Physics and Technology State University, Dolgoprudny, Russia.
- ^m Also at The Collaborative Innovation Center of Quantum Matter (CICQM), Beijing, China.
- ⁿ Also at Università di Napoli Parthenope, Napoli, Italy.
- ^o Also at Institute of Particle Physics (IPP), Canada.
- ^p Also at Horia Hulubei National Institute of Physics and Nuclear Engineering, Bucharest, Romania.
- ^q Also at Department of Physics, St. Petersburg State Polytechnical University, St. Petersburg, Russia.
- ^r Also at Borough of Manhattan Community College, City University of New York, New York City, United States.
- ^s Also at Department of Financial and Management Engineering, University of the Aegean, Chios, Greece.
- ^t Also at Centre for High Performance Computing, CSIR Campus, Rosebank, Cape Town, South Africa.
- ^u Also at Louisiana Tech University, Ruston LA, United States.
- ^v Also at Institutio Catalana de Recerca i Estudis Avancats, ICREA, Barcelona, Spain.
- ^w Also at Graduate School of Science, Osaka University, Osaka, Japan.
- ^x Also at Fakultät für Mathematik und Physik, Albert-Ludwigs-Universität, Freiburg, Germany.
- ^y Also at Institute for Mathematics, Astrophysics and Particle Physics, Radboud University Nijmegen/Nikhef, Nijmegen, Netherlands.
- ^z Also at Department of Physics, The University of Texas at Austin, Austin TX, United States.
- ^{aa} Also at Institute of Theoretical Physics, Ilia State University, Tbilisi, Georgia.
- ^{ab} Also at CERN, Geneva, Switzerland.
- ^{ac} Also at Georgian Technical University (GTU), Tbilisi, Georgia.
- ^{ad} Also at Ochadai Academic Production, Ochanomizu University, Tokyo, Japan.
- ^{ae} Also at Manhattan College, New York NY, United States.
- ^{af} Also at Department of Physics, The University of Michigan, Ann Arbor MI, United States.
- ^{ag} Also at The City College of New York, New York NY, United States.
- ^{ah} Also at Departamento de Física Teórica y del Cosmos, Universidad de Granada, Granada, Portugal.
- ^{ai} Also at Department of Physics, California State University, Sacramento CA, United States.
- ^{aj} Also at Moscow Institute of Physics and Technology State University, Dolgoprudny, Russia.
- ^{ak} Also at Departement de Physique Nucleaire et Corpusculaire, Université de Genève, Geneva, Switzerland.
- ^{al} Also at Institut de Física d'Altes Energies (IFAE), The Barcelona Institute of Science and Technology, Barcelona, Spain.
- ^{am} Also at School of Physics, Sun Yat-sen University, Guangzhou, China.
- ^{an} Also at Institute for Nuclear Research and Nuclear Energy (INRNE) of the Bulgarian Academy of Sciences, Sofia, Bulgaria.
- ^{ao} Also at Faculty of Physics, M.V. Lomonosov Moscow State University, Moscow, Russia.
- ^{ap} Also at National Research Nuclear University MEPhI, Moscow, Russia.
- ^{aq} Also at Department of Physics, Stanford University, Stanford CA, United States.
- ^{ar} Also at Institute for Particle and Nuclear Physics, Wigner Research Centre for Physics, Budapest, Hungary.
- ^{as} Also at Giresun University, Faculty of Engineering, Turkey.
- ^{at} Also at CPPM, Aix-Marseille Université and CNRS/IN2P3, Marseille, France.
- ^{au} Also at Department of Physics, Nanjing University, Jiangsu, China.
- ^{av} Also at Institute of Physics, Academia Sinica, Taipei, Taiwan.
- ^{aw} Also at University of Malaya, Department of Physics, Kuala Lumpur, Malaysia.
- ^{ax} Also at LAL, Univ. Paris-Sud, CNRS/IN2P3, Université Paris-Saclay, Orsay, France.
- * Deceased.